Plant Physiology Preview. Published on June 5, 2015, as DOI:10.1104/pp.114.254466

Subfamily-specific Fluorescent Probes for Cys proteases Display Dynamic Protease Activities During Seed Germination

Haibin Lu[1,2], Balakumaran Chandrasekar[1,2], Julian Oeljeklaus[3], Johana Misas-Villamil[1,2], Zheming Wang[3], Takayuki Shindo[2], Matthew Bogyo[4], Markus Kaiser[3], Renier A. L. van der Hoorn[1,2]

[1] The Plant Chemetics Laboratory, Department of Plant Sciences, University of Oxford, OX1 3RB Oxford, UK

[2] The Plant Chemetics Laboratory, Max Planck Institute for Plant Breeding Research, Cologne, Germany

[3] Center for Medical Biotechnology, Faculty of Biology, University of Duisburg-Essen, 45117 Essen, Germany

[4] Department of Pathology, Stanford School for Medicine, Stanford, CA 94305-5324, USA

Keywords: papain-like cysteine protease, aleurain, cathepsin B, legumain, vacuolar processing enzyme, activity-based protein profiling, protease activity profiling, seed germination

Running title: Selective Cys protease profiling

Cys proteases are an important class of enzymes implicated in both developmental and defence-related programmed cell death and other biological processes in plants. Because there are dozens of Cys proteases that are post-translationally regulated by processing, environmental conditions and inhibitors, new methodologies are required to study these pivotal enzymes individually. Here, we introduce fluorescent activity-based probes that specifically target three distinct Cys protease subfamilies: aleurain-like proteases (ALPs), cathepsin B-like proteases (CTBs), and vacuolar processing enzymes (VPEs). We applied protease activity profiling with these new probes on Arabidopsis protease knock-out lines and agroinfiltrated leaves to identify the probe targets, and on other plant species to demonstrate their broad applicability. These probes revealed that most commercially available protease inhibitors target unexpected proteases in plants. When applied on germinating seeds, these probes reveal dynamic activities of ALPs, CTBs and VPEs, coinciding with the remobilization of seed storage proteins.

Downloaded from www.plantphysiol.org on July 1, 2015 - Published by www.plant.org
Copyright © 2015 American Society of Plant Biologists. All rights reserved.
Copyright 2015 by the American Society of Plant Biologists

INTRODUCTION

Cysteine proteases are a large class of proteolytic enzymes that carry a catalytic cysteine residue in the active site. Plant genomes encode more than 100 cysteine proteases that act in the cytoplasm, the endomembrane system and in the apoplast (Beers et al., 2004; Garcia-Lorenzo et al., 2006; Van der Hoorn et al., 2008; Martinez et al., 2012). Well-studied cysteine proteases include different papain-like cysteine proteases (PLCPs, family C1A of clan CA), vacuolar processing enzymes (VPEs, family C13 of clan CD), metacaspases (MCs, family C14 of clan CD) and multiple families of deubiquitinating enzymes (families 12, 19 and 48 of clans CA and CE).

PLCPs and VPEs have been studied for their role in programmed cell death, both in immunity and development. Tomato Rcr3 and tobacco CathB, for example, are PLCPs required for programmed cell death (PCD) upon pathogen perception (Krüger et al., 2003; Gilroy et al., 2007), whilst Arabidopsis CEP1 and δVPE are pivotal for developmental PCD in pollen and seed coat development, respectively (Nakaune et al., 2005; Zhang et al., 2014). Likewise, Arabidopsis RD21 is a PLCP required for immunity against *Botrytis cinerea* (Shindo et al., 2012; Lampl et al., 2013), whilst its *Nicotiana benthamiana* ortholog C14 contributes to immunity against *Phytophthora infestans* (Kaschani et al., 2010; Bozkurt et al., 2011). Suppression of an aleurain-like PLCP delays floret senescence in Broccoli and increases susceptibility to pathogens in *N. benthamiana* (Eason et al., 2005; Hao et al., 2006) Furthermore, Arabidopsis γVPE is required for toxin-induced PCD whilst its *N. benthamiana* ortholog is required for virus-induced PCD (Kuroyanagi et al., 2005; Hatsugai et al., 2004). In conclusion, these PLCPs and VPEs play different roles, often associated with PCD.

Because of their association with PCD, PLCPs and VPEs are tightly regulated to prevent accidental cell death. Proteases from both families are produced as inactive precursors that require processing in order to remove inhibitory propeptides (e.g. Gu et al., 2012; Kuroyanagi et al., 2002). Furthermore, both classes of proteases are tightly regulated by endogenous inhibitors such as cystatins and serpins (Zhao et al., 2014; Lampl et al., 2013). Because of their post-translational regulations, it is impracticable to predict activities of PLCPs and VPEs from transcript abundance.

New, simple and versatile methods are required to monitor cysteine proteases at their activity level in a broad range of plant species. Protease activity profiling (also called activity-based protein profiling (ABPP) of proteases) is an easy and powerful method to monitor the active state of proteases in crude extracts or living organisms (Willems et al., 2014; Heal et al., 2011; Haedke et al., 2013; Serim et al., 2012). Protease activity profiling is based on the use of chemical probes that react covalently with the active site of proteases in an activity-dependent manner. The result of the labeling is a covalent and irreversible bond between the

Downloaded from www.plantphysiol.org on July 1, 2015 - Published by www.plant.org
Copyright © 2015 American Society of Plant Biologists. All rights reserved.

probe and the protease, which allows subsequent separation on protein gels or purification followed by detection by fluorescence scanning or mass spectrometry.

The first probe that we introduced in plant science was DCG-04, which targets PLCPs (Van der Hoorn et al., 2004). This probe has subsequently been used to monitor PLCP activities during immunity and senescence (Shabab et al., 2008; Martinez et al., 2007a), to study protease activation (Gilroy et al., 2007; Wang et al., 2008; Gu et al., 2012) and to reveal the selectivity of endogenous and pathogen-derived protease inhibitors (Rooney et al., 2005; Tian et al., 2007; Shabab et al., 2008; Lampl et al., 2010; Van Esse et al., 2008; Song et al., 2009; Lozano-Torres et al., 2012; Kaschani et al., 2010; Hörger et al., 2012; Van der Linde et al., 2012; Mueller et al., 2013; Dong et al., 2014). Although powerful, a disadvantage of DCG-04 profiling is that this biotinylated probe involves an indirect detection using streptavidin-HRP, which reduces throughput and resolution. More recently, we introduced fluorescent versions of DCG-04, coined MV201 and MV202 (Richau et al., 2012), and these probes were used to monitor PLCP activities upon herbicide treatment and during PCD in tomato seedlings (Sueldo et al., 2014; Zulet et al., 2013). Unfortunately, however, MV201 and MV202 can cause severe background labeling and their targets can often not be resolved on protein gels because they share the same molecular weight (MW).

More recently, we introduced selective probes for the bacterial effector AvrPphB (Lu et al., 2013) and for VPEs (Misas-Villamil et al., 2013). These probes carry selective targeting peptide sequences to improve their selectivity. The AvrPphB probe (FH11) carries an acidic residue at the second amino acid position preceding the cleavage site (P2=Asp), to mimic substrates of AvrPphB. By contrast, the VPE probe AMS101 carries P2=Pro to prevent cross-reactivity with PLCPs and P1=Asn to specifically target VPEs because these proteases specifically cleave after Asn. These selective probes are much easier to work with and also facilitated *in vivo* imaging of protease labeling sites. For example, FH11 labeling was used to study the proteolytic activation of AvrPphB *in planta*, whilst AMS101 displayed VPE-specific labeling in the vacuole (Lu et al., 2013; Misas-Villamil et al., 2013).

To speed up plant protease research further, we continue to seek better, more selective probes that target specific proteases. Here, we introduce two new specific probes for two subclasses of PLCPs: aleurain-like proteases (ALPs, subclass 8 of the PLCPs), and cathepsin-like proteases (CTBs, subclass 9 of the PLCPs). We also introduce a new, more readily-available probe for VPEs and an improved procedure for PLCP activity profiling with MV202. Using protease mutants, agroinfiltration, VIGS, protease inhibitors and various plant species, we demonstrate the versatility of these probes and illustrate their applicability by characterizing protease activities during seed germination.

Downloaded from www.plantphysiol.org on July 1, 2015 - Published by www.plant.org
Copyright © 2015 American Society of Plant Biologists. All rights reserved.

RESULTS

New Probes for Cys Proteases Light up New Activity Profiles

In this study, we will introduce three new probes and improve the analysis of a previously reported probe (**Fig. 1A**). In addition to the previously used MV202, which targets all PLCPs, we also introduce FY01 and JOGDA1 (**Fig. 1A**) as selective probes that target a subset of PLCPs. Traditionally, names of activity-based probes bear the two initials of chemist who synthesized it (MV, FY or JO), followed by a number or recognizable name. MV202 (Richau et al., 2012) is a biotinylated and fluorescent derivative of the protease inhibitor E-64, which carries a Tyr at the P3 position and a Leu at the P2 position, and an epoxide warhead. FY01 was developed in the Bogyo laboratory as a probe for amino dipeptidyl peptidase I/cathepsin C (Yuan et al., 2008). FY01 carries the non-natural amino acid norvaline (Nle) at the P2 position and homophenylalanine at the P1 position, followed by a vinyl sulfone (VS) reactive group and a Bodipy fluorophore.

JOGDA1 is a bodipy-labeled derivative of FH11, a probe designed for AvrPphB, a secreted papain-like type-III effector produced by *Pseudomonas syringae* (Lu et al., 2013). We re-synthesized FH11 with a stronger bodipy fluorophore to improve the detection of labeled proteins. Besides a bodipy residue, JOGDA1 also carries an acyloxymethylketone (AOMK) reactive group and a Gly-Asp-Ala tripeptide. The Asp residue at the P2 position in FH11 was originally chosen because AvrPphB cleavage requires Asp at P2 of the substrate, which is unique amongst PLCPs that usually prefer a hydrophobic residue at the P2 position of the cleavage site. However, we previously reported that in addition to AvrPphB, FH11 also labels unidentified plant proteins (Lu et al., 2013). Furthermore, we introduce JOPD1 to target legumains/VPEs (**Fig. 1A**), which cleave after Asn and Asp residues. We previously introduced the aza-epoxide-based probe AMS101 for legumains/VPEs (Misas-Villamil et al., 2013). AMS101 is, however, synthetically challenging to produce because of the aza-epoxide reactive group. Chemical synthesis of JOPD1 is much less complicated. JOPD1 is a bodipy version of the PD-AOMK probe described by Sexton et al. (2007) and carries an Asp at the P1 position, whilst the Pro at the P2 position prevents labeling of PLCPs. JOGDA1 and JOPD1 have not been described before and the details of their synthesis is provided (Supplemental **File S1**)

To characterize the targets of MV202, FY01, JOGDA1 and JOPD1, Arabidopsis leaf extracts were labeled at pH 3-9 and the labeled proteins were separated on a protein gel and detected by fluorescence scanning. MV202 labeling causes a large number of signals that increase in intensity at higher pH, especially at pH 8.0 and pH 9.0 (**Fig. 1B**). Importantly, most labeling is not blocked upon pre-incubation with E-64, indicating that these signals are not specific. However, clear signals are detected at 25, 35 and 40 kDa that are absent upon pre-incubation with E-64. These signals show an optimum intensity at slightly acidic pH (pH

Downloaded from www.plantphysiol.org on July 1, 2015 - Published by www.plant.org
Copyright © 2015 American Society of Plant Biologists. All rights reserved.

5-6). pH 6.0 was chosen for further studies because of the strongest detection of 25 and 35 kDa signals.

FY01 labeling causes two close strong signals at 34 kDa, that is absent upon pre-incubation with E-64 and have a maximum intensity at neutral pH (pH 6-8) (**Fig. 1B**). At higher pH, unspecific labeling occurs increasingly. This unspecific labeling is less strong at pH 8.0 when compared to that caused by MV202. FY01 also displays labeling of a specific 40 kDa signal at acidic pH (pH 5.0), which is presumably identical to the signal caused at 40 kDa by MV202. We therefore chose pH 7.0 to display the specific 34 kDa signal.

JOGDA1 labeling displays a weak but specific 34 kDa signal at pH 5-8 (**Fig. 1B**), which sometimes displays as a doublet on high resolving protein gels. JOGDA1 labeling causes very low unspecific labeling at higher pH. No other specific signals are displayed with this probe. pH 6.0 was chosen for further studies, since this caused the strongest labeling in repeated labeling experiments.

Finally, JOPD1 labeling shows signals only at pH 4.0 and pH 5.0 and low unspecific labeling at higher pH (**Fig. 1B**). The signals consist of two 40 kDa signals and a weaker 35 kDa signal. Labeling can be prevented upon preincubation with caspase-1 inhibitor Ac-YVAD-cmk (YVAD), but not E64 (**Fig. 1C**). pH 5.0 was chosen for subsequent labeling experiments since the signal is strongest at this pH.

A direct comparison of the labeled proteins on one gel shows that the signals have overlapping MWs at 40 kDa (MV202 and JOPD1) and 34 kDa (MV202, FY01 and JOGDA1) (**Fig. 1C**). This figure also shows that unspecific labeling is strongest for MV202, causing strong signals at 40 kDa and higher that are not suppressed upon preincubation with E-64.

Improved Broad-range Fluorescent Profiling of MV202-labeled Proteomes

The strong, unspecific labeling profile of MV202 was unexpected. MV202 has previously only been used on apoplastic proteomes of tomato and on leaf extracts of agroinfiltrated *N. benthamiana* (Richau et al., 2012; Sueldo et al., 2014). These MV202-labeled proteomes did not show strong background signals and the few detected signals are specific because they are absent upon preincubation with E-64. We hypothesized that the background labeling is caused by unspecific reaction of the excess MV202 probe when heated up in gel loading buffer before loading. To test this hypothesis, we labeled leaf proteomes with and without MV202 and then followed three different work-up procedures. Acetone precipitation to remove the excess unlabeled probe does not prevent fluorescent background labeling (**Fig. 2A**). However, acetone precipitation followed by a purification of biotinylated proteins on avidin beads causes four specific signals of 25-30 kDa (**Fig. 2B**). By contrast, purification without acetone precipitation still causes background labeling (**Fig. 2C**). Taken together, these data indicate that the background labeling is caused by the presence of excess probe that reacts

Downloaded from www.plantphysiol.org on July 1, 2015 - Published by www.plant.org
Copyright © 2015 American Society of Plant Biologists. All rights reserved.

unspecifically with proteins when not removed by precipitation and purification. For the remaining labeling assays with MV202 described in this manuscript, samples were precipitated and purified to prevent background labeling.

Protease Mutants Identify Different Specific Probe Targets

Because the signals detected by MV202, FY01 and JOGDA1 are blocked by preincubation with E-64 (**Fig. 1B**), we anticipate that these probes target PLCPs. Likewise, we anticipate that JOPD1 targets legumains/VPEs because the labeling is blocked upon preincubation with Ac-YVAD-cmk but not E-64 (**Fig. 1B**). We therefore took advantage of Arabidopsis PLCP and VPE mutant collections (Wang et al., 2008; Gruis et al., 2004) to determine the targets of these probes by screening for the absence of labeling. In addition to the single PLCP and VPE mutants, we included double, triple and quadruple protease mutants. Only protease mutants that show altered labeling profiles are presented here.

Labeling of leaf extracts of protease mutants with MV202 indicated the identity for each of the four signals. The bottom two signals are absent in the *aalp-1* null mutant (**Fig. 3A,** signals 3 and 4), indicating that these signals represent AALP. This is consistent with previous data that this region contains AALP protein upon DCG-04 labeling (Van der Hoorn et al., 2004). These bottom signals were also absent in the *aalp-1* mutant using DCG-04 labeling (Gu et al., 2012). Likewise, the top signal (signal 1) is reduced in both the *rd21A-1* and *ctb3-1* mutants (**Fig. 3A**), indicating that this signal contains RD21 and CTB3, in agreement with previous data were RD21 and CTB3 were identified in this region (Van der Hoorn et al., 2004). We believe that the top signal caused an accumulation of both labeled RD21 and CTB3 and not by activation of CTB3 by RD21 or *vice versa*, because CTB3 labeling is normal in *rd21A-1* mutants (see below) and RD21 processing, accumulation and activity is unaltered in the *ctb3-1* mutant (Supplemental **Figure S1**). The second top signal (signal 2) is absent in the *ctb3-1* mutant (**Fig. 3A**), indicating that this signal is caused by CTB3.

Significantly, labeling of the PLCP mutants revealed that both FY01 signals are absent in the *aalp-1* mutant (**Fig. 3A,** signals 5 and 6), indicating that FY01 labels AALP. This is surprising because the MW of the FY01 signals (ca. 34 kDa) is larger than the bottom *AALP*-dependent signals detected upon MV202 labeling (ca. 25 kDa, **Fig. 3A**, signals 3 and 4). Thus, when labeled with FY01, AALP runs at a larger apparent MW than when labeled with MV202, which is opposite to the expected based on the MW of the probes themselves (1.0 and 1.4 kDa, respectively, **Fig. 1A**). However, selective AALP labeling by FY01 can be explained by the fact that this probe was designed to target aminodipeptidases (Yuan et al., 2008). AALP is a cathepsin H-like aminopeptidase because of the presence of a covalently linked minichain that is retained in the substrate binding groove to prevent endopeptidase

Downloaded from www.plantphysiol.org on July 1, 2015 - Published by www.plant.org
Copyright © 2015 American Society of Plant Biologists. All rights reserved.

activity (Guncar et al., 1998). The detection of two *AALP*-dependent FY01 signals is consistent with the earlier observation that AALP accumulates as two mature isoforms on Western blots probed with the anti-AALP antibody (Ahmed et al., 2000).

Importantly, the mutant screen also revealed that both signals generated by JOGDA1 labeling are absent in the *ctb3-1* mutant (**Fig. 3A,** signals 7 and 8), indicating that JOGDA1 targets CTB3. This is also the region where CTB3 has been identified by mass spectrometry (Van der Hoorn et al., 2004), and where MV202 labels two *CTB3*-dependent signals (**Fig. 3A**, signals 1 and 2). The labeling of CTB3 by JOGDA1 is surprising since this probe carries an Asp at the P2 position, which was thought to exclude PLCP labeling. That CTB3 may exist in two isoforms was not reported before.

Finally, to investigate targets for JOPD1, we included the quadruple *vpe* (*qvpe*) mutant, lacking all four VPEs (Gruis et al., 2004). The JOPD1 signals are absent in this *qvpe* mutant (**Fig. 3A,** signals 9 and 10), indicating that JOPD1 indeed labels VPEs. This labeling profile is consistent with the occurrence of various active isoforms of γVPE, the most abundant VPE in leaves (Kuroyanagi et al., 2002; Misas-Villamil et al., 2013). The absence of PLCP labeling by JOPD1 is caused by the fact that PLCPs do not bind peptides with a P2=Pro residue.

In conclusion, the absence of labeling on mutant plants shows that probe targets are not active in the mutants. At this stage, it is yet unclear if this is caused by the absence of the protease itself, or indirectly caused by removal of a protease that is required to activate the protease that is labeled.

Transient Protease Expression Confirms Labeling of Respective Proteases

To confirm that the new probes label the different Cys proteases, we transiently expressed CTB3, AALP, ALP2 and all four VPEs by agroinfiltration of *Nicotiana benthamiana* and labeled extracts from agroinfiltrated leaves with the respective activity-based probes at the chosen labeling conditions. Specific signals were detected upon labeling of leaves expressing CTB3 with JOGDA1, confirming that JOGDA1 labels CTB3 (**Fig. 3B**). This signal was absent in leaves where CTB3 was not expressed, and in case CTB3 containing extracts were pre-incubated with E-64. The 34 kDa signal has the same MW as the *CTB3*-dependent JOGDA1 signal detected in Arabidopsis leaf extracts, indicating that the Arabidopsis 34 kDa signal originates from CTB3 labeling. Interestingly, an additional, strong 38 kDa signal appeared when CTB3-containing extracts were labeled with JOGDA1. This signal was also detected upon MV201 labeling (Richau et al., 2012), and is possibly caused by labeling of the proenzyme of CTB3.

Specific signals were also detected when extracts from leaves transiently expressing *AALP* and *ALP2* were labeled with FY01 (**Fig. 3B**), confirming that this probe indeed labels

Downloaded from www.plantphysiol.org on July 1, 2015 - Published by www.plant.org
Copyright © 2015 American Society of Plant Biologists. All rights reserved.

both aleurain-like proteases of Arabidopsis. These signals were absent upon pre-incubation with E-64 and from leaves that do not express AALP or ALP2. Different from the calculated MW of mature AALP and ALP2 proteases (23.7 and 24.0 kDa, respectively), both proteases migrate at a larger MW (33 and 34 kDa) than expected, and AALP migrates at a slightly lower MW than ALP2. The AALP signal is nevertheless consistent with the AALP-dependent FY01 signal at 34 kDa in Arabidopsis leaf extracts, indicating that this signal originates from AALP. ALP2 is not expressed in leaves but is detected in leaves (see below).

Finally, fluorescent signals were also detected when extracts from leaves transiently expressing VPEs were labeled with JOPD1 (**Fig. 3C**), confirming that all four VPEs can be labeled with JOPD1. These signals are absent upon pre-incubation with the VPE inhibitor YVAD-cmk, and different for extracts not expressing Arabidopsis VPEs, confirming that VPE labeling is specific. The labeling profiles are polymorphic for the different VPEs, and consistent with described VPE isoforms and labeling with AMS101 (Kuroyanagi et al., 2002; Misas-Villamil et al., 2013).

In conclusion, these labeling assays on mutant plants and agroinfiltrated leaves show that the three new probes label different subfamilies of Cys proteases: FY01 labels aleurain-like proteases (ALPs, e.g. AALP), JOGDA1 targets cathepsin-B-like proteases (CTBs, e.g. CTB3), and JOPD1 targets vacuolar processing enzymes (VPEs).

Distinct Protease Activity Profiles in Different Plant Species

To demonstrate that our probes are broadly applicable in plant science, we profiled protease activities in leaf extracts of different (model) plant species, including *Solanaceae* (winter cherry, tomatillo, tomato and tobacco) and monocots (barley and maize). Preincubation with E-64 or YVAD-cmk was used to demonstrate the specificity of labeling. Detection of fluorescently labeled proteins from protein gels revealed specific signals in all leaf extracts and with all probes that are absent upon pre-incubation with the respective inhibitors (**Fig. 4A-D**), illustrating that labeling with our new probes is broadly applicable. The profiles, however, are remarkably different in MW and intensities. These differences are probably caused by different number of protease genes and different protein processing in the different species. In general, FY01 and JOGDA1 signals correspond to the signals in the MV202 activity profiles, although MV202 labeling profiles are often too weak to display all the signals. Also, as with Arabidopsis labeling, FY01 signals migrate considerably slower in the protein gel than the presumed MV202-labeled counterparts. Thus, FY01 and JOGDA1 labeling facilitates the deconvolution of otherwise weak or overlapping and complicated activity profiles generated by MV202 labeling. Notable is also the observation that unspecific labeling by FY01 and JOGDA1 occurs more in leaf extracts of some plants (e.g. Arabidopsis and barley), even though the same amount of protein was labeled.

Downloaded from www.plantphysiol.org on July 1, 2015 - Published by www.plant.org
Copyright © 2015 American Society of Plant Biologists. All rights reserved.

To independently confirm the selective labeling of ALPs and CTBs in *N. benthamiana*, we silenced aleurain-like protease (*NbALP*, NbS00032309g0011.1) and cathepsin-B protease (*NbCTB*, NbS00035145g0007.1) in *Nicotiana benthamiana* using virus-induced gene silencing (VIGS). Labeling of leaf extracts of *N. benthamiana* with MV202, FY01 and JOGDA1 causes very similar, overlapping signals, in both unchallenged plants (**Fig. 4ABC**), as well as in *TRV::GFP* plants (**Fig. 4E**). Labeling of leaf extracts from protease silenced plants, however, revealed that FY01 labeling is only suppressed in *TRV::NbALP*, whereas JOGDA1 labeling is only suppressed in *TRV::NbCTB* plants (**Fig. 4E**). These data confirm that also in *N. benthamiana*, FY01 and JOGDA1 selectively label ALPs and CTBs, respectively. These data illustrate the strength of using selective probes to monitor specific proteases on other plant species.

Selective Chemical Interference of Proteases using Inhibitors

Equipped with the new, selective Cys protease probes, we tested if we can use these probes to determine the selectivity of commercially available protease inhibitors. We assembled a collection of 13 protease inhibitors that can potentially inhibit Cys proteases. The collection contains caspase inhibitors YVAD-cmk and DEVD-cmk, proteasome inhibitors MG132 and MG115, PLCP inhibitors E-64, antipain, chymostatin and leupeptin, and Cathepsin-B inhibitors LVK-cho and zFA-cmk. We also included three custom-made inhibitors (**Fig. 5A**). JCP410 is an inhibitor of dipeptidyl dipeptidase I (DPPI)/Cathepsin C (Arastu-Kapur et al., 2008), consisting of an Nle-Phe dipeptide with a vinyl sulfone reactive group, similar to the warhead of the FY01 probe. We also synthesized JOGDA2, which contains a Pro-Asp dipeptide with an AOMK reactive group that is similar to the JOPD1 probe for legumains/VPEs, except that JOGDA2 carries an alkyne minitag instead of the bodipy fluorophore. Finally, we synthesized JOPD2, which consists of a Gly-Asp-Ala tripeptide and an AOMK reactive group, similar to the warhead of the fluorescent FH11 and JOGDA1 probes. All these inhibitors will covalently and irreversibly react with the active site Cys residues of the proteases with the exception of the aldehyde-based inhibitors (MG132, MG115, antipain, chymostatin, LVK-cho and leupeptin), which covalently but reversibly bind to the substrate binding groove.

Leaf extracts were pre-incubated with 50 µM of the putative protease inhibitors and then incubated with the different probes to label the non-inhibited enzymes. The labeling profiles revealed a surprising diversity of inhibitory activities. In general, suppression of AALP labeling was consistent between MV202 and FY01 labeling (**Fig. 5B**). Most importantly, these experiments demonstrate a lack of presumed selectivity of commercially available inhibitors. Proteasome inhibitors MG132 and MG115 also block both AALP and CTB3 labeling, but not VPE labeling (**Fig. 5B**), consistent with our previous observation that

Downloaded from www.plantphysiol.org on July 1, 2015 - Published by www.plant.org
Copyright © 2015 American Society of Plant Biologists. All rights reserved.

MG132 blocks PLCP activities *in vivo* (Kaschani et al., 2009). In addition, cathepsin-B inhibitors LVK-cho and zFA-cmk also block AALP and RD21 labeling, but not VPE labeling (**Fig. 5B**), consistent with previous observations (Gilroy et al., 2007). Likewise, caspase inhibitors YVAD-cmk and DEVD-cho also block CTB3 labeling (**Fig. 5B**). Importantly, YVAD-cmk but not DEVD-cho also blocks VPE labeling (**Fig. 5B**), consistent with notion that VPEs have caspase-1 but not caspase-3 activity (Hatsugai et al., 2004; Rojo et al., 2004; Misas-Villamil et al., 2013). These data illustrate that commercially available inhibitors with claimed specificity should be used on plants with extreme caution. By contrast, our new custom-made inhibitors indicate the desired selective inhibition: JCP410 selectively blocks AALP labeling, displayed using both MV202 and FY01 (**Fig. 5B**). Likewise, JOPD2 selectively blocks VPE labeling displayed with JOPD1 (**Fig. 5B**). Unexpectedly, JOGDA2 is not selective as it suppresses AALP labeling in addition to CTB3 labeling (**Fig. 5B**). Thus, these data indicate that inhibitors JCP410, DEVD-cho and JOPD2 can be used for selective inhibition of activities of AALP, CTB3 and VPEs, respectively.

Dynamic Protease Activities during Seed Germination

Seed germination is an important phase transition for plants that involves a the degradation seed storage proteins, releasing products that are used to build Rubisco (Ribulose-1,5-biphosphate carboxylase/oxygenase) and other proteins (**Fig. 6A**). Notably, the proteases that are active during seed germination and possibly responsible for the conversion of the seed proteome have not been described before. Here, we investigated protease activities during germination of Arabidopsis seeds using our specific fluorescent probes. The conversion of the seed proteome is clearly visible when the proteomes are separated on protein gels (**Fig. 6A**). The 12 S globulins that cause four signals at 25-35 kDa and two signals at 15-20 kDa are degraded during germination, whilst rubisco large subunit (RBCL) and other proteins appear (**Fig. 6A**).

The seed extracts were labeled with specific probes to monitor protease activities. FY01 labeling of extracts of germinating seeds revealed no signals in imbibed seeds (day 0) that were blocked upon pre-incubation with E-64 and three signals of 30 kDa that appears at day 1 (signal 1), day 2 (signal 2) and day 3 (signal 4) and a weak signal of 40 kDa appearing at day 3 (signal 3) (**Fig. 6B**). All these FY01 signals were suppressed upon pre-incubation with E-64. JOGDA1 labeling revealed two signals of 30 kDa appearing at day 1 (signal 1) and day 2 (signal 2), that were absent upon pre-incubation with E-64, but no signals in extracts from imbibed seeds (**Fig. 6C**). Finally, JOPD1 labeling displays five signals in imbibed seeds in the regions of 40 kDa (signals 1-3) and 25 kDa (signals 4 and 5), of which signal 1 increases in intensity during seed germination, whilst signal 4 and 5 decrease in intensity (**Fig. 6D**). All these JOPD1 signals were absent upon pre-incubation with YVAD-cmk. These

Downloaded from www.plantphysiol.org on July 1, 2015 - Published by www.plant.org
Copyright © 2015 American Society of Plant Biologists. All rights reserved.

assays illustrate a dynamic change in protease activities during seed germination in Arabidopsis.

Protease Mutants Reveal Identities of Protease Activities during Seed Germination

We next used protease mutants to annotate the signals in these activity profiles. Importantly, while doing this, we did not detect any alteration in the conversion of seed storage proteins (data not shown), indicating that none of these proteases is individually essential for seed storage protein degradation.

To identify the FY01 signals during germination, we tested various PLCP mutant seeds. FY01 signals 1, 3 and 4 are absent in the mutants *alp2-1*, *rd21-1* and *aalp-1*, respectively (**Fig. 7A**), indicating that they represent ALP2, RD21 and AALP, respectively. Importantly, labeling of RD21 demonstrates that FY01 does not exclusively label ALPs, but can incidentally also label other Cys proteases at pH 7. FY01 signal 2 is absent in the *aalp-1* mutant and must be caused by AALP at day 2, but its identity remains unclear at day 3 (**Fig. 7A**). These data indicate that ALP2 activity appears at day 1 and AALP and RD21 activity at day 2. These activities correlate with the transcript levels measured for the corresponding genes during germination (Narsai et al., 2011, **Fig. 7B**).

We next identified the JOGDA1 signals using single, double and triple *ctb* mutant seeds. JOGDA1 signal 2 is absent in the *ctb3-1* mutants, indicating that it is caused by CTB3 (**Fig. 7C**). JOGDA1 signal 1 is also absent in the *ctb3-1* mutant at day 1, indicating that it is caused by CTB3 (**Fig. 7C**). At later time points, however, signal 1 is reduced in the *ctb3-1* mutant and absent in the *ctb2-1/ctb3-1* double mutants (*ctb2/3*), indicating that this signal consists of CTB2 and CTB3 at days 2 and 3. All signals are absent in the *ctb2-1/ctb3-1* double mutant and the *#62-5* triple mutant (**Fig. 7C**). These data indicate that CTB3 activity appears at day 1 and CTB2 activity follows at day 2. The relative intensities correlate with relative transcript levels: *CTB3* is highly expressed, followed by *CTB2*, whereas *CTB1* is poorly expressed (**Fig. 7D**). More interestingly, *CTB2* and *CTB3* transcript levels are constitutively high, whereas their activity only appears at 1 and 2 days after imbibition. The absence of CTB activity in the presence of *CTB* transcript indicates that CTBs are subject to post-transcriptional regulation to suppress their activity at early time points.

Finally, we identify the JOPD1 signals using the single, double and triple *vpe* mutant seeds (Gruis et al., 2002; 2004). JOPD1 signal 1 is absent in the *αvpe* mutant and in the *αβδvpe* triple and *qvpe* quadruple mutants (**Fig. 7E**), indicating that this signal is caused by αVPE. Signals 2-5 are all absent in the *βvpe* mutant (**Fig. 7E**), indicating that all these signals are caused by βVPE. Interestingly, there is a weak signal 2 remaining in the *βvpe*, *βδvpe* and *αβδvpe* mutants that is absent in the *qvpe* quadruple mutant (**Fig. 7E**), indicating that this

Downloaded from www.plantphysiol.org on July 1, 2015 - Published by www.plant.org
Copyright © 2015 American Society of Plant Biologists. All rights reserved.

signal is caused by γVPE. The dominance of βVPE in the JOPD1 activity profile correlates with the fact that the *βVPE* gene has relatively high transcript levels (**Fig. 7F**). Surprisingly, however, is the fact that αVPE is clearly detected (signal 1 in **Fig. 7E**), whilst the *αVPE* transcript level is relatively low (**Fig. 7F**). By contrast, γVPE activity is barely detectable (Signal 2 in **Fig. 7E**), but the *γVPE* transcript levels are significantly higher when compared to *αVPE* (**Fig. 7F**). The transcript data used here (extracted from Narsai et al., 2011), is consistent with *VPE* transcript data presented by Gruis et al. (2004). Taken together, these data indicate that there are several cases during seed germination where the activity level of proteases can not be predicted from the transcript data.

DISCUSSION

Using fluorescent gel imaging and Arabidopsis protease mutants, we have validated the specificity of new fluorescent probes for protease activity profiling in plants. We provide proof-of-concept on leaf extracts of other plant species and on germinating Arabidopsis seeds. We also used these probes to reveal unexpected selectivity of commercially available protease inhibitors and have found several examples where protease activities do not correspond with transcript levels, highlighting the relevance of this technology to display a new level of functional proteomic information.

The four probes target different cysteine proteases at different pH. The pH sensitivity is explained by the fact that proteases have pH-dependent activities. Aleurains, for example, show optimal activities at pH 6.5-7.0 (Holwerda & Rogers, 1992), whereas VPEs have an optimal activity at pH 5.0 (Kuroyanagi et al., 2002). These optimal pH values likely reflect the microenvironment conditions at which these proteases function.

That PLCPs are labeled with MV202 was shown before and is expected because this probe is based on E-64, which inhibits PLCPs broadly (Richau et al., 2012). Likewise, JOPD1 targets VPEs because they carry an Asp residue at the P1 position, which at low pH is protonated, thereby mimicking an Asn residue for which VPEs are selective (Kato et al., 2005). The additional P2=Pro prevents labeling of PLCPs, which prefer hydrophobic residues at this positions. Similar probes carrying a Pro-Asp dipeptide and an AOMK warhead were previously used to label mammalian legumains, which are orthologous to VPEs (Sexton et al., 2007).

Unexpected probe targets were found for FY01 and JOGDA1. FY01 was developed as a specific probe for mammalian Cathepsin C, also called dipeptidyl peptidase I (DPPI, Yuan et al., 2008), but this enzyme does not have a close homolog in plants (**Fig. S1**). Instead, FY01 labels aleurains, which are orthologous to mammalian Cathepsin H proteases (Richau et al., 2012, **Fig. S2**). Although slightly unexpected, the selectivity is explained by the fact that

Downloaded from www.plantphysiol.org on July 1, 2015 - Published by www.plant.org
Copyright © 2015 American Society of Plant Biologists. All rights reserved.

aleurains and Cathepsin H proteases carry a peptide minichain that blocks part of the substrate binding groove, thereby preventing endoprotease activity (Guncar et al., 1998). Because of this minichain, the unprimed substrate binding groove accommodates only two residues, explaining why aleurains cleave two residues from the N-terminus and are called aminodipeptidases. Labeling of aleurains by FY01 is explained because FY01 caries two amino-terminal residues adjacent to the vinyl sulfone reactive group.

A second unexpected probe target is the selective labeling of CTBs by JOGDA1. JOGDA1 was designed to selectively target AvrPphB by carrying P2=Asp. This probe should not label PLCPs because they prefer a hydrophobic residue at this position. Surprisingly, our data indicates that, in contrast to other plant PLCPs, CTBs can accommodate acidic residues at the P2 position, hence explaining the selectivity of JOGDA1. Importantly, selective labeling of leaf extracts of other plant species indicated that these properties of ALPs and CTBs are universal, as confirmed by silencing experiments in *N. benthamiana*.

Although FY01 preferentially labels ALPs, we did notice that FY01 also labels 40 kDa Cys proteases at lower pH (**Fig. 1B**) and in seedling extracts (**Fig. 7A**). This 40 kDa signal is probably caused by labeling of RD21A, as the signal is absent in seedlings of *rd21A-1* mutants. By contrast, JOGDA1 and JOPD1 show selective labeling of CTBs and VPEs, respectively, and we did not detect labeling of other proteins. Thus, caution is needed for the interpretation of FY01 labeling. To confirm the specificity of labeling one can: (i) knock out/down the corresponding protease to show that labeling dissapears; (ii) purify and identify by mass spectrometry; or (iii) characterize labeling further, by studying sensitivity for inhibitors, pH, cofactors, etc. A similar approach was used to characterize VPEs in the apoplast of infected tomato plants (Sueldo et al., 2014).

Besides specific labeling, which can be blocked upon preincubation with a corresponding inhibitor, we also noted strong unspecific labeling of the probes at increasingly high pH. The level of this unspecific labeling is different between the probes and is possibly caused by the different reactive groups. Epoxide-based MV202 causes strong background labeling at pH 8-9; the vinyl sulfone probe FY01 causes background labeling at pH 9.0, and very low background labeling was displayed by JOGDA1 and JOPD1, which both carry acyloxymethylketone reactive groups. We also noticed that the intensity of background labeling can depend on the plant species (**Fig. 4**) and on the type of subcellular extract (data not shown). We have shown that background labeling can be prevented by precipitation and purification of labeled proteins using probes that carry both a fluorescent group and a biotin affinity handle. We speculate that this unspecific labeling is caused by unspecific labeling of unreacted probes during the heating of the sample in SDS sample buffer.

Using FY01 and JOGDA1 labeling instead of MV202 labeling has several advantages. First, these probes cause much less background labeling and are therefore much easier to

Downloaded from www.plantphysiol.org on July 1, 2015 - Published by www.plant.org
Copyright © 2015 American Society of Plant Biologists. All rights reserved.

handle. Second, these probes display different protease classes that are difficult to discriminate by MV202 profiling because of their overlapping MW. This may not be so clear for Arabidopsis leaf extracts because Arabidopsis AALP and CTB3 have a different MW, but this is different for other plant species where the MV202 signals overlap. These studies also readily revealed that monocots may carry multiple CTB isoforms.

Further studies with selective protease probes revealed that commercially available protease inhibitors often have unexpected selectiveness. This is problematic since many pharmacological studies using these inhibitors in plants have implied the involvement of particular proteases. These conclusions should be carefully reconsidered. Frequently used proteasome inhibitors MG115 and MG132, for example, also inhibit ALPs and CTBs, whereas CTB inhibitors LVK-cho and zFA-cmk also inhibit other PLCPs. However, inhibitors can be remarkably selective for the proteases that we were testing, illustrated by the seeming specific inhibition of ALPs, CTBs and VPEs by JCP410, DEVD-cho and JOGDA2, respectively. It should be noted, however, that our data do not exclude that the selective inhibitors also inhibit other proteins that we are not monitoring. More characterized inhibitors can be used for chemical knock-out assays to study the role of proteases in plants even if they are not genetic model species.

Protease activity profiling of germinating seeds revealed that the activation of ALPs and CTBs correlates with the remobilization of storage proteins. Although their involvement in seed storage processing seems likely, our data did not demonstrate the involvement of ALPs and CTBs in protein remobilization because the remobilization is unaltered in the protease mutants, and even in the ALP double and CTB triple mutants (data not shown). Redundancy is, however, common for plant proteases as illustrated by the redundancy of the VPEs in the processing of seed storage proteins during seed ripening (Gruis et al., 2004; Shimada et al., 2003).

Although some protease activities correlate with transcript levels, others do clearly not. CTB2 and CTB3, for example, are transcribed in seeds, but their activity is undetected until day 1 and day 2, implicating that the activities of these CTBs are suppressed at early stages of seed germination. One unconfirmed candidate for CTB regulation is AtCYS6, a cystatin that is expressed in seeds and disappears during germination (Hwang et al., 2009). AtCYS6 knock-out mutants germinate faster, implicating a role for AtCYS6 in protease regulation during seed germination (Hwang et al., 2009). It will be interesting to determine if CTB2/3 activities are increased in the AtCYS6 mutants and if AtCYS6 can suppress labeling of CTB2/3 using competitive ABPP (Song et al., 2009; Kaschani et al., 2010; Dong et al., 2014).

We also noted that αVPE causes strong activity signals in germinating seeds, whilst γVPE is relative weak, in contrast to their relative expression level. This observation

Downloaded from www.plantphysiol.org on July 1, 2015 - Published by www.plant.org
Copyright © 2015 American Society of Plant Biologists. All rights reserved.

implicates that VPE activities are also post-transcriptionally and/or post-translationally regulated during seed germination, perhaps also through AtCYS6 or AtCYS7, which both carry a C-terminal extension, known to inhibit VPEs (Martinez et al., 2007b). Interestingly, whilst AtCYS6 is expressed in seeds and disappears during germination, AtCYS7 is co-expressed with γVPE (Supplemental **Fig. S3**). A similar post-translational protease regulation by cystatins has been hypothesized for germinating barley seeds (Martinez et al., 2009). The tight regulation of proteases by cystatins has also been demonstrated in tobacco embryos (Zhao et al., 2013), illustrating the need to monitor these protease activities individually to unravel their functions.

MATERIALS AND METHODS

Activity-based probes and inhibitors – The synthesis of FY01, MV202 and JCP410 have been described before (Arastu-Kapur et al., 2008; Yuan et al., 2008; Richau et al., 2012). The synthesis of JOGDA1, JOPD1, JOGDA2 and JOPD2 are described in the supplemental information (Supplemental **File S1**). Protease inhibitors E-64, Ac-YVAD-cmk, MG132, MG115, antipain, chymostatin and leupeptin were purchased from Sigma-Aldrich and Ac-DEVD-cho, Ac-LVK-cho and zFA-cmk from Calbiochem. Synthesized probes and inhibitors are available upon request.

Arabidopsis mutants - The following Arabidopsis mutants have been used in this study: *rd21A-1* (SALK_090550), *aalp-1* (SALK_075550); *ctb3-1* SALK_019630; *ctb1-2* SALK_110946 (Wang et al., 2008); *#62-5* (McLellan et al., 2009) and *αvpe, βvpe, γvpe, δvpe, βδvpe, αβδvpe, and qvpe* (Gruis et al., 2004). The *alp2-1* mutant (SALK_079981) and *ctb2-1* mutant (SALK_089030), have been selected for this study using primers flanking the T-DNA insertion site (5'-tctgtcgactattgag-3' and 5'-ttgtggatcttgttggac-3'; 5'-cgttggtcacacatagtgcag-3' and 5'-gacaatactggttgctcgcac-3', respectively) and the LBa1 primer 5'-tggttcacgtagtgggccatcg-3'. The *ctb3-1/ctb2-1* double mutant was generated by crossing, and the *rd21-1/aalp-1* double mutant has been reported before (Gu et al., 2012). Arabidopsis plants were grown at 22°C (day)/20°C (night) in a glass house under a 16 h light regime. Leaves from rosettes of 6-week old Arabidopsis plants were used for the protein extraction.

Agroinfiltration – Leaves of *Nicotiana benthamiana* that transiently express proteases were prepared as described before (Richau et al., 2012; Misas-Villamil et al., 2013), using binary plasmids pFK16(*35S::CTB3*), pFK17(*35S::AALP*), pHL7(*35S::ALP2*), pFK137(*35S::αVPE*), pFK138(*35S::βVPE*), pFK139(*35S::γVPE*) and pFK140 (*35S::δVPE*). pFK16, 17 and 137-140 have been described before (Richau et al., 2012; Misas-Villamil et al., 2013). pHL7 was constructed similarly as described before (Shabab et al., 2008) by cloning a PCR fragment amplified using primers 5'-tgcattcccaagtcccaac -3' and 5'-agctccatggctgtgaaactaaacctatcttcctc -3' from Arabidopsis cDNA into pFK26 using NcoI and

Downloaded from www.plantphysiol.org on July 1, 2015 - Published by www.plant.org
Copyright © 2015 American Society of Plant Biologists. All rights reserved.

PstI restriction sites, resulting in pHL6. The *35S::ALP2* expression cassette was shuttled from pHL6 into pTP5 using XbaI and SalI restriction sites. Agrobacterium cultures (OD=1.0) carrying binary plasmid encoding the silencing inhibitor p19 were mixed (1:1) with and without Agrobacterium carrying a binary plasmid encoding the different proteases and agroinfiltrated into expanded leaves of 4-week old *N. benthamiana* plants. At day four after agroinfiltration, six leaf disks (each 1 cm diameter) were ground in 600 µL extraction buffer containing 1% polyvinylpolypyrrolidone (PVPP) and 2 mM dithiotreitol (DTT). The pH of the extraction buffer was pH 5.0 (for VPEs), pH 6.0 (for CTBs) or pH 7.0 (for ALPs). The extract was cleared by centrifugation and the supernatant pre-incubated for 30 minutes with or without 50 µM E-64 or YVAD-cmk and labeled for 4 hours with 2 µM of the respective probes. Labeled proteins were detected by in-gel fluorescent scanning.

Other plant species – Other plant species were grown under normal greenhouse conditions and samples were taken from adult, expanded leaves. Proteins were extracted in 2 mM DTT. For *N. benthamiana* and *N. tabacum*, 5% PVPP was added before protein extractions. Protein concentrations were measured and normalized before labeling.

Virus-induced gene silencing – TRV::NbALP and *TRV::NbCTB* were generated by cloning a 300 bp fragment of NbS0032309g0011.1 (*NbALP*) and NbS00035145g0007.1 (*NbCTB*) using primers 5'-gatcggatccgaggtacgagacagttgaggag-3', 5'-gatcgaattcccagcaagatccgcacttgccctgg-3', 5'-gatcggatccggccggatggaaagctgcactg-3' and 5'-gatcgaattcttgctgacagagagatattcaagcc-3', resulting in pTS9 (*TRV::NbALP*) and pTS7 (*TRV::NbCTB*), respectively. Overnight-grown *Agrobacterium tumefaciens* cultures (strain GV3101) carrying plasmids pTS7 and pTS9 were resuspended in infiltration buffer (10 mM MES pH 5.0, 10 mM $MgCl_2$, and 1 mM acetosyringone). The optical density at 600 nm was adjusted to 2, and cultures carrying pTS7 and pTC9 were mixed with cultures carrying the *TRV1* vector. Cultures were incubated for 3 hr at room temperature in the dark, and infiltrated into the first two true leaves of two-week-old *N. benthamiana* plants. Total proteins were extracted from upper leaves after three weeks and used for labeling.

Seed germination – Arabidopsis seeds were sterilized and plated on 1/2 MS medium (2.15 g/L MS medium, Duchefa M0221) containing 1% Agar. Seeds were imbibed on the 1/2 MS agar plates for two days at 4 ºC in the dark. The agar plates were incubated at 20-22 °C under 16 h light regime for seed germination. Seeds were collected at day 0, 1, 2 and 3 post imbibition and frozen at -80 ºC until protein extraction.

Leaf protein extraction and labeling - 600 µl of extraction buffer containing 50 mM sodium acetate (for pH 6.0 and below) or 50 mM Tris-HCl (for pH 7.0 and above) and 2 mM DTT were added to six leaf discs (1.0 cm diameter) of *Arabidopsis thaliana* in a 1.5 ml tube. After grinding the tissues with blue stick, the samples were centrifuged at 10,000g, 4ºC for 10 min and the supernatant containing the soluble proteins was used for labeling. Labeling was

Downloaded from www.plantphysiol.org on July 1, 2015 - Published by www.plant.org
Copyright © 2015 American Society of Plant Biologists. All rights reserved.

performed in a 50 µl total volume. 45 µl of leaf extracts (containing ~100 µg soluble proteins) were pre-incubated with 50 µM E-64 or Ac-YVAD-cmk for 30 minutes at room temperature. These extracts were incubated with 2 µM MV202 or JOPD1, or 0.06 µM FY01 or 5 µM JOGDA1 for 4h at room temperature in the dark. Equal volumes of DMSO were added for no-probe-controls.

Seed protein extraction and labeling- Proteins were extracted by grinding the seeds in sterilized water. The samples were centrifuged at 10000 g, 4ºC for 10 min and the supernatant containing the soluble proteins was used for labeling. Labeling was performed in a 50 µl format. 45 µl of seed extracts (containing ~50 µg soluble proteins) were pre-incubated with 50 µM E-64 at pH 6.0 (MV202 or JOGDA1) or pH 7.0 (FY01) or 50 µM Ac-YVAD-cmk at pH 5.0 (JOPD1) or DMSO for 30 minutes at room temperature. These extracts were incubated with 2 µM FY01, JOGDA1 or JOPD1 for 4h at room temperature in the dark. Equal volumes of DMSO were added to the no-probe-control.

Improved MV202 labeling – 50-100 µg leaf extract was preincubated with or without 50 µM E-64 (or other commercial protease inhibitors) in 500 µL total volume containing 50 mM Tris (pH 6.0) and 2 mM DTT at room temperature for 30 min, then 1 µL 1mM MV202 (or DCG-04) was added. The samples were kept on the rotator in the dark at room temperature for 4 hrs. The samples were precipitated by adding 1 mL ice-cold cold acetone and centrifuging at 4 ºC at 10,000g for 5 min, and washed with 70% cold acetone once. Protein pellets were resuspended in 50 mM Tris-HCl (pH 7.0) containing 10 µL Avidin agarose (Sigma) beads. Samples were incubated with the beads at room temperature for 1 hr and the beads were washed by 1% SDS twice and heated for 5 min at 95ºC in 50 µL SDS gel loading buffer.

Analysis of labeled proteins - The labeling reactions were stopped by adding gel loading buffer containing β-mercaptoethanol at 1X final concentration and heating at 95ºC for 5 minutes. The labeled proteins were separated on 12% protein gels at 200 volts for one hour. The labeled proteins were detected from the protein gels with a Typhoon FLA 9400 scanner (Amersham Biosciences / GE Healthcare) using excitation wavelength at 532 nm and the 580 nm band-pass filter (580BP30).

Bioinformatics – transcript levels published by Narsai et al. (2011) were extracted from the NCBI Gene Expression Omnibus (GEO) dataset GSE30223 using GEO2R. The phylogenetic tree of human PLCPs (Lecaille et al., 2002) and Arabidopsis PLCPs (Richau et al. 2012) was made by Cluster Omega (Sievers et al., 2011).

ACKNOWLEDGEMENTS

We would like to thank Hermen Overkleeft and Martijn Verdoes for providing MV202 and DCG-04, Leonard Both for mining Genevestigator data and Adriana Pruzinska for technical

Downloaded from www.plantphysiol.org on July 1, 2015 - Published by www.plant.org
Copyright © 2015 American Society of Plant Biologists. All rights reserved.

assistance. This work was financially supported by the Max Planck Society, ERA-IB project 'Produce', COST CM1004 'Chemical Proteomics', the University of Oxford and an ERC Starting grant (grant No. 258413 to M.K.) and Consolidator grant (grant No. 616449 'GreenProteases' to RvdH).

LITERATURE CITED

Ahmed SU, Rojo E, Kovaleva V, Venkataraman S, Dombrowski JE,Matsuoka K, Raikhel NV (2000) The plant vacuolar sorting receptor AtELP is involved in transport of NH(2)-terminal propeptide-containing vacuolar proteins in *Arabidopsis thaliana*. J Cell Biol **149**: 1335–1344

Arastu-Kapur S, Ponder EL, Fonovic UP, Yeoh S, Yuan F, Fonovic M, Grainger M Phillips CI, Powers JC, Bogyo M (2008) Identification of proteases that regulate erythrocyte rupture by the malaria parasite *Plasmodium falciparum*. Nat Chem Biol **4**: 203-213

Beers EP, Jones AM, Dickerman AW (2004) The S8 serine, C1A cysteine and A1 aspartic protease families in Arabidopsis. Phytochemistry **65**: 43-58

Bozkurt T, Schornack S, Win J, Shindo T, Ilyas M, Oliva R, Cano LM, Jones AME, Huitema E, Van der Hoorn RAL, Kamoun S (2011) *Phytophthora infestans* effector AVRblb2 prevents secretion of a plant immune protease at the haustorial interface. Proc Natl. Acad Sci USA **108**: 20832-20837

Dong S, Stam R, Cano LM, Song J, Sklenar J, Yoshida K, Bozkurt TO, Oliva R, Liu Z, Tian M, Win J, Banfield MJ, Jones AM, Van der Hoorn RAL, Kamoun S (2014) Effector specialization in a lineage of the Irish potato famine pathogen. Science **343**: 552-555

Eason JR, Ryan DJ, Watson LM, Hedderley D, Christey MC, Braun RH, Couple SA (2005) Suppression of the cysteine protease, aleurain, delays floret senescence in *Brassica oleracea*. Plant Mol Biol **57**: 645-657

Garcia-Lorenzo M, Sjödin A, Jansson S, Funk C (2006) Protease gene families in Populus and Arabidopsis. BMC Plant Biol. **6**: 30

Gilroy E, Hein I, Van der Hoorn R, Boevink P, Venter E, McLellan H, Kaffarnik F, Hrubikova K, Shaw J, Holeva M, Lopez E, Hidalgo O, Pritchard L, Loake G, Lacomme C, Birch P (2007) Involvement of cathepsin B in the plant disease resistance hypersensitive response. Plant J **52**: 1-13

Gruis DF, Selinger DA, Curran JM, Jung R (2002) Redundant proteolytic mechanisms process seed storage proteins in the absence of seed-type members of the vacuolar processing enzyme family of cysteine proteases. Plant Cell **14**: 2863-2882

Gruis DF, Schulze J, Jung R (2004) Storage protein accumulation in the absence of the vacuolar processing enzyme family of cysteine proteases. Plant Cell **16**: 270-290

Gu C, Shabab M, Strasser R, Wolters PJ, Shindo T, Niemer M, Kaschani F, Mach L, Van der Hoorn RAL (2012) Post-translational regulation and trafficking of the granulin-containing protease RD21 of Arabidopsis thaliana. PLoS One **7**: e32422

Guncar G, Podobnik M, Pungercar J, Strukelj B, Turk V, Turk D (1998) Crystal structure of porcine cathepsin H determined at 2.1 A resolution: location of the mini-chain C-terminal carboxyl group defines cathepsin H aminopeptidase function. Structure **6**: 51-61

Headke U, Küttler E, Vosyka O, Yan Y, Verhelst SHL (2013) Tuning probe selectivity for chemical proteomics applications. Curr Opin Chem Biol **17**: 102-10

Hao L, Hsiang T, Goodwin PH (2006) Role of two cysteine proteinases in the susceptible response of *Nicotiana benthamiana* to *Colletotrichum destructivum* and the hypersensitive response to *Pseudomonas syringae* pv. *tomato.* Plant Science **170**: 1001-1009

Downloaded from www.plantphysiol.org on July 1, 2015 - Published by www.plant.org
Copyright © 2015 American Society of Plant Biologists. All rights reserved.

Hatsugai N, Kuroyanagi M, Yamada K, Meshi T, Tsuda S, Kondo M, Nishimura M, Hara-Nishimura I (2004) A plant vacuolar protease, VPE, mediates virus-induced hypersensitive cell death. Science **305**: 855–858

Heal WP, Dang THT, Tate EW (2011) Activity-based probes: discovering new biology and new drug targets. Chem Soc Rev **40**: 246-257

Holwerda BC, Rogers JC (1992) Purification and characterization of aleurain: a plant thiol protease functionally homologous to mammalian cathepsin H. Plant Physiol **99**: 848-855

Hörger AC, Ilzas M, Stephan W, Tellier A, Van der Hoorn RAL, Rose LE (2012) Balancing selection at the tomato RCR3 guardee gene family maintains variation in strength of pathogen defense. PLoS Genetics **8**: e1002813

Hwang JE, Hong JK, Je JH, Lee KO, Kim DY, Lee SY, Lim CO (2009) Regulation of seed germination and seedling growth by an Arabidopsis phytocystatin isoform, AtCYS6. Plant Cell Rep **28**: 1623-1632

Kaschani F, Shabab M, Bozkurt T, Shindo T, Schornack S, Gu C, Ilyas M, Win J, Kamoun S, Van der Hoorn RAL (2010) An effector-targeted protease contributes to defense against *Phytophthora infestans* and is under diversifying selection in natural hosts. Plant Physiol **154**: 1794-1804

Kuroyanagi M, Nishimura M, Hara-Nishimura I (2002) Activation of Arabidopsis vacuolar processing enzyme by self-catalytic removal of an auto-inhibitory domain of the C-terminal propeptide. Plant Cell Physiol. **43**: 143-151

Kaschani F, Verhelst SHL, Van Swieten PF, Verdoes M, Wong CS, Wang Z, Kaiser M, Overkleeft HS, Bogyo M, Van der Hoorn RAL (2009) Minitags for small molecules: detecting targets of reactive small molecules in living plant tissues using 'click-chemistry'. Plant J **57**: 373-385

Kato D, Boatright KM, Berger AB, Nazif T, Blum G, Ryan C, Chehade KAH, Salvesen G, Bogyo M (2005) Activity based probes that target diverse cysteine protease families. Nat. Chem Biol **1**: 33–38

Krüger J, Thomas CM, Golstein C, Dixon MS, Smoker M, Tang S, Mulder L, Jones JDG (2002) A tomato cysteine protease required for *Cf-2*-dependent disease resistance and suppression of autonecrosis. Science **296**: 744–747

Kuroyanagi M, Nishimura M, Hara-Nishimura I. (2002) Activation of Arabidopsis vacuolar processing enzyme by self-catalytic removal of an auto-inhibitory domain of the C-terminal propeptide. Plant Cell Physiol **43**: 143–151

Kuroyanagi M, Yamada K, Hatsugai N, Kondo M, Nishimura M, Hara-Nishimura I (2005) Vacuolar processing enzyme is essential for mycotoxin-induced cell death in *Arabidopsis thaliana.* J Biol Chem **280**: 32914–32920

Lampl N, Budai-Hadrian O, Davydov O, Joss TV, Harrop SJ, Curmi PMG, Roberts TH, Fluhr R (2010) Arabidopsis AtSerpin, crystal structure and in vivo interaction with its target protease responsive to desiccation-21 (RD21*).* J Biol Chem **285**: 13550–13560

Lampl N, Akan N, Fluhr R (2013) Set-point control of RD21 protease activity by AtSerpin1 controls cell death in Arabidopsis. Plant J **74**: 498-510

Lecaille F, Kaleta J, Bromme D (2002) Human and parasitic papain-like cysteine proteases: their role in physiology and pathology and recent developments in inhibitor design. Chem Rev **102**: 4459-4488

Lozano-Torres JL, Wilbers RHP, Gawronski P, Boshoven JC, Finkers-Tomczak A, Cordewener JHG, America AHP, Overmars HA, Van 't Klooster JW, Baranowski L, Sobczak M, Ilzas M, Van der Hoorn RAL, Schots A, De Wit PJGM, Bakker J, Goverse A, Smant G (2012) Dual *Cf-2*-mediated disease resistance in tomato requires a common virulence target of a fungus and a nematode. Proc Natl Acad Sci USA **109**: 10119-10124

Lu H, Wang Z, Shabab M, Oeljeklaus J, Verhelst SH, Kaschani F, Kaiser M, Bogyo M, Van der Hoorn RA L (2013) A substrate-inspired probe monitors translocation, activation and subcellular targetting of bacterial type III effector protease AvrPphB. Chem Biol **20**: 168-176

Martinez M, Cambra I, Gonzalez-Melendi P, Santamaria ME, Diaz I (2012) C1A cysteine-proteases and their inhibitors in plants. Physiol. Plant **145**: 85-94

Downloaded from www.plantphysiol.org on July 1, 2015 - Published by www.plant.org
Copyright © 2015 American Society of Plant Biologists. All rights reserved.

Martinez DE, Bartoli CG, Grbic V, Guiamet JJ (2007a) Vacuolar cysteine proteases from wheat (*Triticum aestivum* L.) are common to leaf senescence induced by different factors. J Exp Bot **58**: 1099-1107

Martinez M, Diaz-Mendoza M, Carrillo L, Diaz I (2007b) Carboxy terminal extended phytocystatins are bifunctional inhibitors of papain and legumain cysteine proteinases. FEBS Lett **581**: 2914-2918

Martinez M, Cambra I, Carrillo L, Diaz-Mendoza M, Diaz I (2009) Characterization of the entire gene family in barley and their target cathepsin L-like cysteine-proteases, partners in the hordein mobilization during seed germination. Plant Physiol **151**: 1531-1545

McLellan H, Gilroy EM, Yun BW, Birch PRJ, Loake GJ (2009) Functional redundancy in the Arabidopsis Cathepsin B gene family contributes to basal defence, the hypersensitive response and senescence. New Phytologist **183**: 408-418

Misas-Villamil JC, Toenges G, Kolodziejek I, Sadaghiani AM, Kaschani F, Colby T, Bogyo M, Van der Hoorn RA L (2013) Activity profiling of vacuolar processing enzymes reveals a role for VPE during oomycete infection. Plant J **73**: 689-700

Mueller AN, Ziemann S, Treitschke S, Assmann D, Doehlemann G (2013) Compatibility in the *Ustilago maydis*-maize interaction requires inhibition of host cysteine proteases by the fungal effector Pit2. PLoS Pathog **9**: e100377

Nakaune S, Yamada K, Kondo M, Kato T, Tabata S, Nishimura M, Hara-Nishimura I (2005) A vacuolar processing enzyme, delta-VPE, is involved in seed coat formation at the early stage of seed development. Plant Cell **17**: 876–887

Narsai R, Law SR, Carrie C, Whelan J (2011) In-depth temporal transcriptome profiling reveals a crucial developmental switch with roles for RNA processing and organelle metabolism that are essential for germination in Arabidopsis. Plant Physiol **157**: 1342-1362

Richau K, Kaschani F, Verdoes M, Pansuriya TC, Niessen S, Stüber K, Overkleeft HS, Bogyo M, Van der Hoorn RAL (2012) Subclassification and biochemical analysis of plant papain-like cysteine proteases displays subfamily-specific characteristics. Plant Physiol **158**: 1583-1599

Rojo E, Martin R, Carter C, Zouhar J, Pan S, Plotnikova J, Jin H, Panegue M, Sanchez-Serrano JJ, Baker B, Ausubel FM, Raikhel NV (2004) VPEgamma exhibits a caspase-like activity that contributes to defense against pathogens. Curr Biol **14**: 1897–1906

Rooney H, Van 't Klooster J, Van der Hoorn RAL, Joosten MHAJ, Jones JDG, De Wit PJGM (2005) Cladosporium Avr2 inhibits tomato Rcr3 protease required for *Cf-2*-dependent disease resistance. Science **308**: 1783-1789

Serim S, Haedke U, Verhelst SHL (2012) Activity-based probes for the study of proteases: recent advances and developments. ChemMedChem **7**: 1146-1159

Sexton KB, Witte MD, Blum G, Bogyo M (2007) Design of cell-permeable, fluorescent activity-based probes for the lysosomal cysteine protease asparaginyl endopeptidase (AEP)/legumain. Bioorg Med Chem Lett **17**: 649-653

Shimada T, Yamada K, Kataoka M, Nakaune S, Koumoto Y, Kuroyanagi M, Tabata S, Kato T, Shinozaki K, Seki M, Kobayashi M, Kondo M, Nishimura M, Hara-Nishimura I (2003) Vacuolar processing enzymes are essential for proper processing of seed storage proteins in *Arabidopsis thaliana.* J Biol Chem **278**: 32292-32299

Shabab M, Shindo T, Gu C, Kaschani F, Pansuriya T, Chintha R, Harzen A, Colby T, Kamoun S, Van der Hoorn RAL (2008) Fungal effector protein AVR2 targets diversifying defence-related Cys proteases of tomato. Plant Cell **20**: 1169-1183

Shindo T, Misas-Villamil JC, Hörger A, Song J, Van der Hoorn RAL (2012) A role in immunity for Arabidopsis cysteine protease RD21, the ortholog of the tomato immune protease C14. PLoS One **7**: e29317

Sievers F, Wilm A, Dineen D, Gibson TJ, Karplus K, Li W, Lopez R, McWilliam H, Remmert M, Soding J, Thompson JD, Higgins DG (2011) Fast, scalable generation of high-quality protein multiple sequence alignments using Clustal Omega. Mol Syst Biol **7**: 539

Downloaded from www.plantphysiol.org on July 1, 2015 - Published by www.plant.org
Copyright © 2015 American Society of Plant Biologists. All rights reserved.

784 **Song J, Win J, Tian M, Schornack S, Kaschani F, Muhammad I, Van der Hoorn RAL,**
785 **Kamoun S** (2009) Apoplastic effectors secreted by two unrelated eukaryotic plant
786 pathogens target the tomato defense protease Rcr3. Proc Natl Acad Sci USA **106**: 1654-1659
787 **Sueldo D, Ahmed A, Misas-Villamil J, Colby T, Tameling W, Joosten MHAJ, Van der**
788 **Hoorn RAL** (2014) Dynamic hydrolase activities precede hypersensitive tissue collapse in
789 tomato seedlings. New Phytologist **203**: 913-925
790 **Tian M, Win J, Song J, Van der Hoorn R, Van der Knaap E, Kamoun S** (2007) A
791 *Phytophthora infestans* cystatin-like protein interacts with and inhibits a tomato papain-like
792 apoplastic protease. Plant Physiol **143**, 364-277
793 **Van der Hoorn RAL** (2008) Plant proteases: from phenotypes to molecular mechanisms.
794 Annu Rev Plant Biol **59**: 191–223
795 **Van der Hoorn RAL, Leeuwenburgh MA, Bogyo M, Joosten MHAJ, Peck SC** (2004)
796 Activity profiling of papain-like cysteine proteases in plants. Plant Physiol **135**: 1170-1178
797 **Van der Linde K, Hemetsberger C, Kastner C, Kaschani F, Van der Hoorn RAL,**
798 **Kumlehn J, Doehlemann G** (2012) A maize cystatin suppresses host immunity by
799 inhibition of apoplastic cysteine proteases. Plant Cell **24**: 1285-1300
800 **Van Esse HP, Van't Klooster JW, Bolton MD, Yadeta KA, Van Baarlen P, Boeren S,**
801 **Vervoort J, De Wit, PJGM, Thomma PBHJ** (2008) The *Cladosporium fulvum* virulence
802 protein AVR2 inhibits host proteases required for basal defence. Plant Cell **20**: 1948-1963
803 **Wang Z, Gu C, Colby T, Shindo T, Balamurugan R, Waldmann H, Kaiser M, Van der**
804 **Hoorn RAL** (2008) Beta-lactone probes identify a papain-like peptide ligase in *Arabidopsis*
805 *thaliana.* Nat Chem Biol **4:** 557-563
806 **Willems LI, Overkleeft HS, Van Kasteren SI** (2014) Current developments in activity-
807 based protein profiling. Bioconj Chem **25**: 1181-1191
808 **Yuan F, Verhelst SHL, Blum G, Coussens LM, Bogyo M** (2008) A selective activity-based
809 probe for the papain family cysteine protease dipeptidyl peptidase I/Cathepsin C. J Am
810 Chem Soc **128**: 5616-5617
811 **Zhang D, Liu D, Lv X, Wang Y, Xun Z, Liu Z, Li F, Lu H** (2014) The cysteine protease
812 CEP1, a key executor involved in tapetal programmed cell death, regulates pollen
813 development in Arabidopsis. Plant Cell **26**: 2939-2961
814 **Zhao P, Zhou XM, Zhang LY, Wang W, Ma, LG, Yang LB, Peng XB, Bozhkov PV, Sun,**
815 **MX** (2013) A bipartite molecular module controls cell death activation in the basal cell
816 lineage of plant embryos. PLoS Biol **11**: e10011655
817 **Zulet A, Gil-Monreal M, Villamor JG, Zabalza A, Van der Hoorn RAL, Royuela**
818 **M** (2013) Proteolytic pathways induced by herbicides that inhibit amino acid
819 biosynthesis. PLoS One **8**: e73847
820

Downloaded from www.plantphysiol.org on July 1, 2015 - Published by www.plant.org
Copyright © 2015 American Society of Plant Biologists. All rights reserved.

LEGENDS

Figure 1. Novel probes display new, pH-dependent labelling profiles.

(A) Structural components of the novel Cys protease probes. Each of the four probes contains a dipeptide or tripeptide that targets into the P3, P2 and P1 substrate binding pockets in the different proteases. All probes carry a bodipy fluorescent reporter group (Bp, yellow). MV202 also contains a biotin affinity tag (B, blue). The reactive groups (red) are either epoxide, vinyl sulphone (VS) or acyloxymethylketone (AOMK). FY01 carries an N-terminal dipeptide to capture aminodipeptidases.

(B) Labeling of PLCPs is pH-dependent. Leaf extracts were pre-incubated at pH 3-9 with or without 50 µM E-64/YVAD and then labeled with 2 µM MV202, FY01 or JOGDA1. Dashed lines indicate selected labeling conditions.

(C) Compared labelling profiles on Arabidopsis leaf extracts. Leaf extracts were pre-incubated with or without 50 µM E-64 or Ac-YVAD-cmk and then labeled with 2 µM probe at pH 5.0 (JOPD1), pH 6.0 (MV202 and JOGDA1) or pH 7.0 (JOPD1).

(B-C) Samples were separated on protein gels and analyzed by fluorescent scanning and coomassie (CBB) staining.

Figure 2. Improved detection by purification of MV202-labeled proteins.

Arabidopsis leaf extracts were labeled with and without DCG04 or MV202. After labeling the samples were either precipitated in acetone **(A)**; precipitated and purified on avidin beads **(B)**; or directly purified on avidin beads **(C)**. Samples were separated on protein gels and analyzed by fluorescent scanning and coomassie (CBB) staining.

Figure 3. Protease knock-out mutants and transient expression reveal specific probe targets in leaf extracts.

(A) Leaf extracts from wild-type Col-0 plants, or from *aalp-1*, *rd21-1*, *ctb3-1* or quadruple *VPE* (*qvpe*) mutants were labelled with MV202, FY01, JOGDA1 or JOPD1 for three hours under the appropriate labelling conditions. Labelled proteomes were separated on protein gels and analysed by in-gel fluorescent scanning and coomassie (CBB) staining.

(B) Extracts of *Nicotiana benthamiana* leaves transiently expressing different proteases were preincubated with 50 µM E-64 (E) or YVAD-cmk (Y) and labeled with FY01, JOGDA1 or JOPD1 with the appropriate labeling conditions. Labelled proteomes were separated on protein gels and analysed by fluorescent scanning and coomassie staining.

Figure 4. Labelling leaves of different plant species illustrates broad applicability

(A-D) Leaf extracts were generated and pre-incubated with 50 (A,B) or 100 (C) µM E-64 or 50 µM JOGDA2 for 30 minutes and then labeled with 2 µM MV202 (A), FY01 (B), JOPD1

Downloaded from www.plantphysiol.org on July 1, 2015 - Published by www.plant.org
Copyright © 2015 American Society of Plant Biologists. All rights reserved.

(D) or 5 µM JOGDA1 (C) for 3 hours. Proteins were separated on protein gels and scanned for fluorescence and stained with coomassie. *Pi, Physalis ixocarpa* (tomatillo); *Sp, Solanum pseudocapsicum* (winter cherry); *At, Arabidopsis thaliana*; *Sl, Solanum lycopersicum* (tomato); *Nt, Nicotiana tabacum* (tobacco); *Nb, Nicotiana benthamiana*; *Hv, Hordeum vulgare* (barley); *Zm, Zea mays* (maize).

(E) Knock-down of *NbALP* and *NbCTB* gene expression in *N. benthamiana* confirms specific labelling. Young plants were inoculated with *TRV::GFP*, *TRV::NbALP* or *TRV::NbCTB* and three weeks later, proteomes were extracted from the upper leaves from two different plants (hence the duplicate) and labelled with FY01 or JOGDA1. Labelled proteomes were separated on protein gels and analysed by fluorescent scanning and coomassie staining.

Figure 5. Commercial and custom-made protease inhibitors display unexpected specificities.

A) Structures of JCP410, and custom-made JOGDA2 and JOPD2.

B) Specific protease inhibition by small molecules. Leaf extracts were pre-incubated for 30 minutes with 50 µM inhibitors and then labelled with MV202, FY01, JOGDA1 or JOPD1 for three more hours. Labelled proteomes were separated on protein gels and analysed by fluorescent scanning and coomassie staining. *, peptide aldehyde.

Figure 6. Dynamic protease activities during seed germination

(A) Proteome conversion during seed germination. Proteins were extracted from germinating seeds at different time points in duplicated and detected on coomassie-stained protein gels.

(B-D) Dynamics of protease activities during germination. Protease activities were displayed by labeling protein extracts with FY01 (B), JOGDA1 (C) and JOPD1 (D).

(A-D) Seeds were imbibed for two days on agar plates for two days at 4°C in the dark, and germinated in 16 h/day light for three days.

Figure 7. Protease mutants elucidate activity profiles in germinating seeds.

Seeds of wild-type and proteases mutant Arabidopsis plants were imbibed and germinated on plates and samples were taken at 0, 1, 2, and 3 days post imbibition. Protein extracts of the seed(ling)s were labelled with FY01 **(A)**, JOGDA1 **(C)** or JOPD1 **(D)** at the appropriate conditions and labelled proteins were detected from protein gels by in-gel fluorescence scanning. **(B, D, E)** Transcript levels of protease genes in imbibed seeds (day 0), and one and two days post imbibition. Data were extracted from Narsai et al. (2011).

Downloaded from www.plantphysiol.org on July 1, 2015 - Published by www.plant.org
Copyright © 2015 American Society of Plant Biologists. All rights reserved.

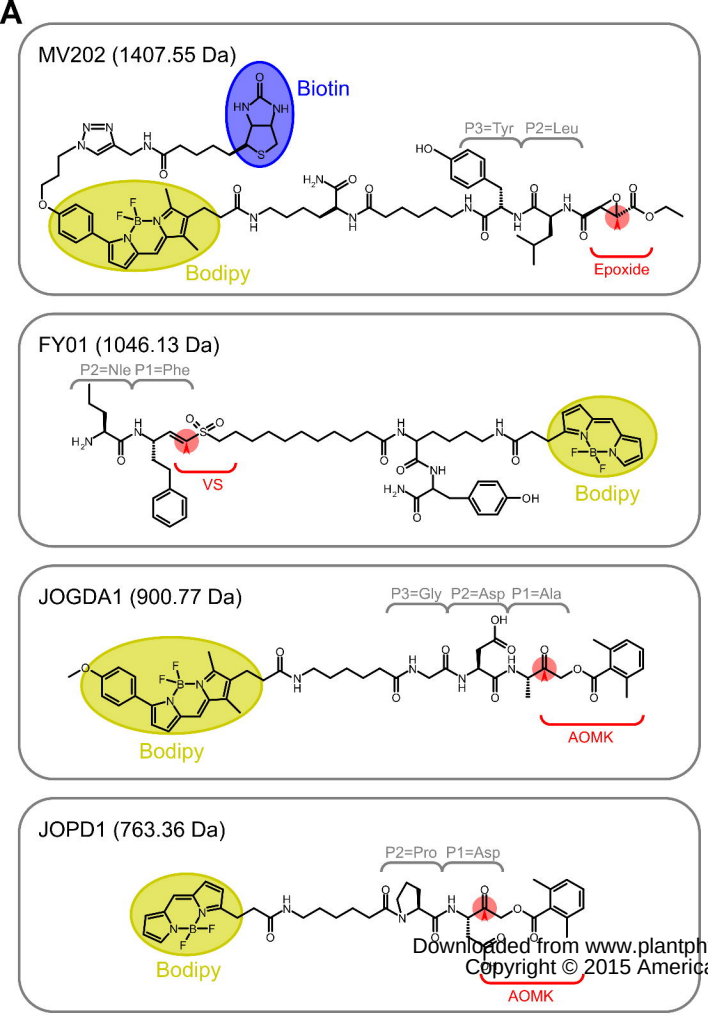

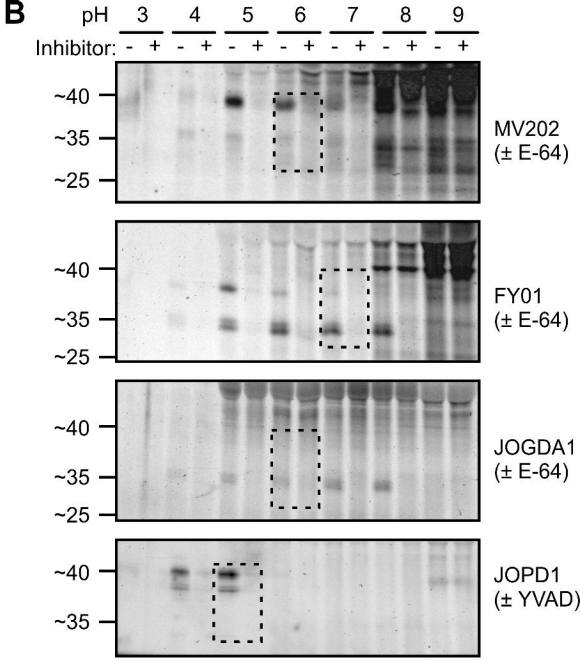

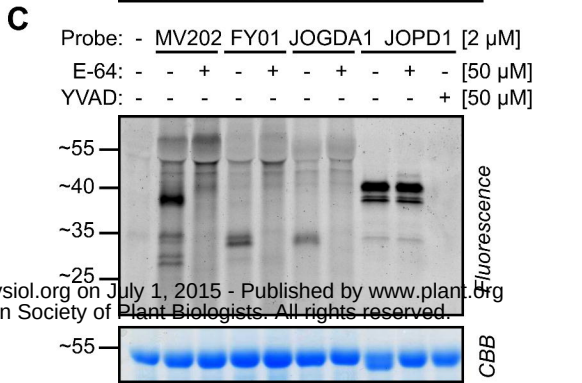

Downloaded from www.plantphysiol.org on July 1, 2015 - Published by www.plant.org
Copyright © 2015 American Society of Plant Biologists. All rights reserved.

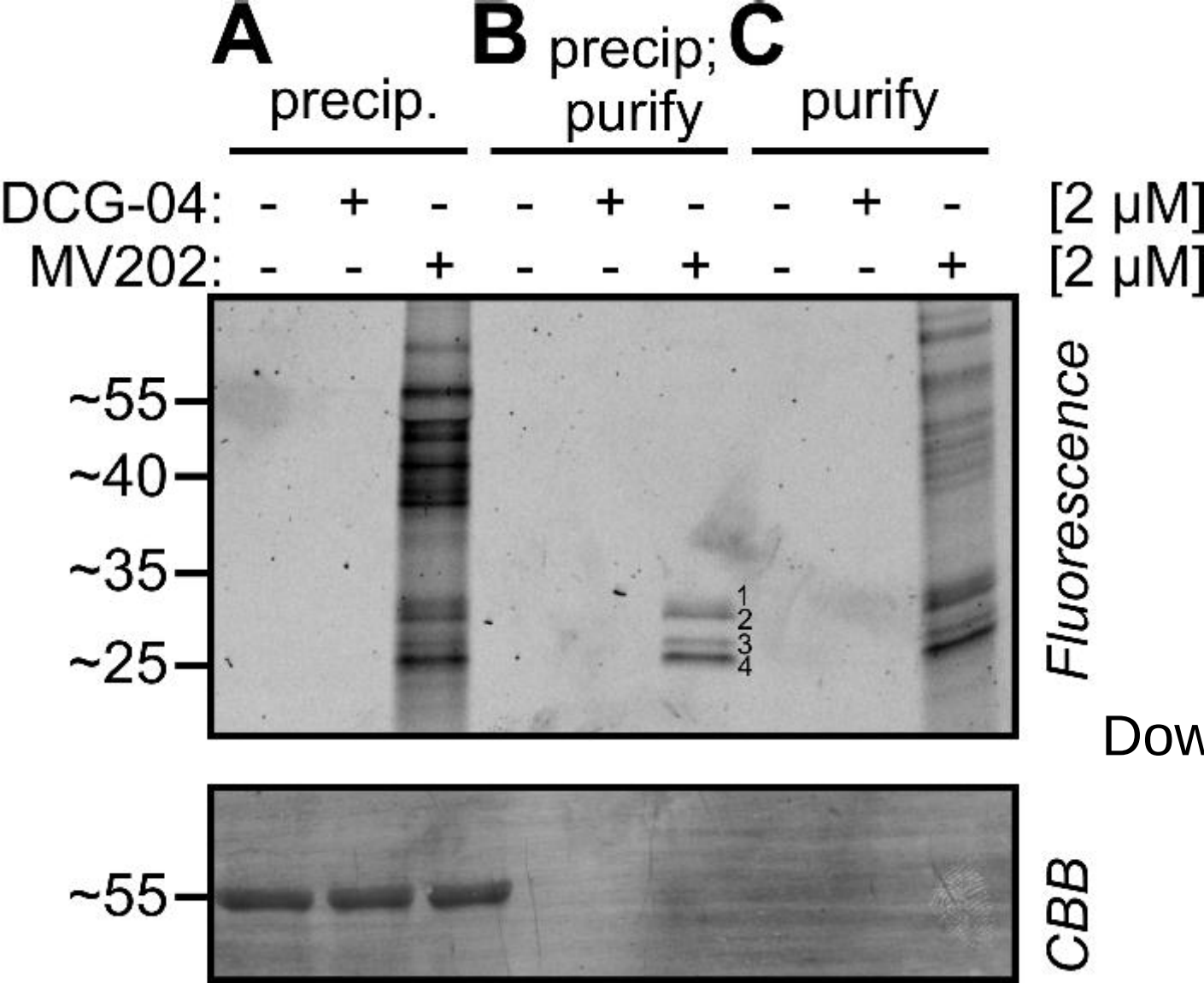
A
precip.
B
precip; purify
C
purify
DCG-04: - + - - + - - + - [2 μM]
MV202: - - + - - + - - + [2 μM]
~55
~40
~35
~25
1
2
3
4
Fluorescence
~55
CBB

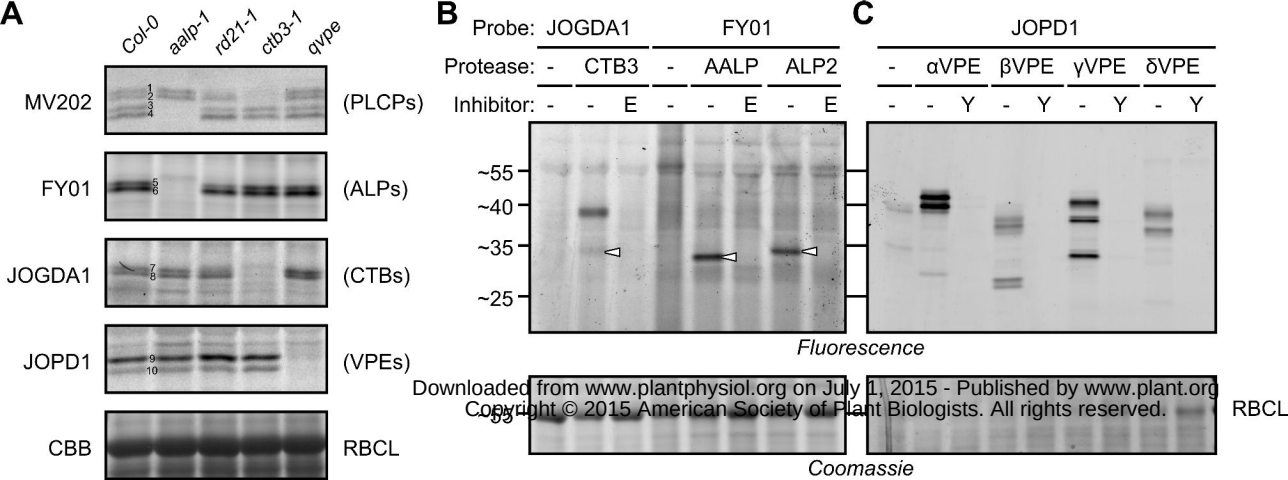

Downloaded from www.plantphysiol.org on July 1, 2015 - Published by www.plant.org
Copyright © 2015 American Society of Plant Biologists. All rights reserved.

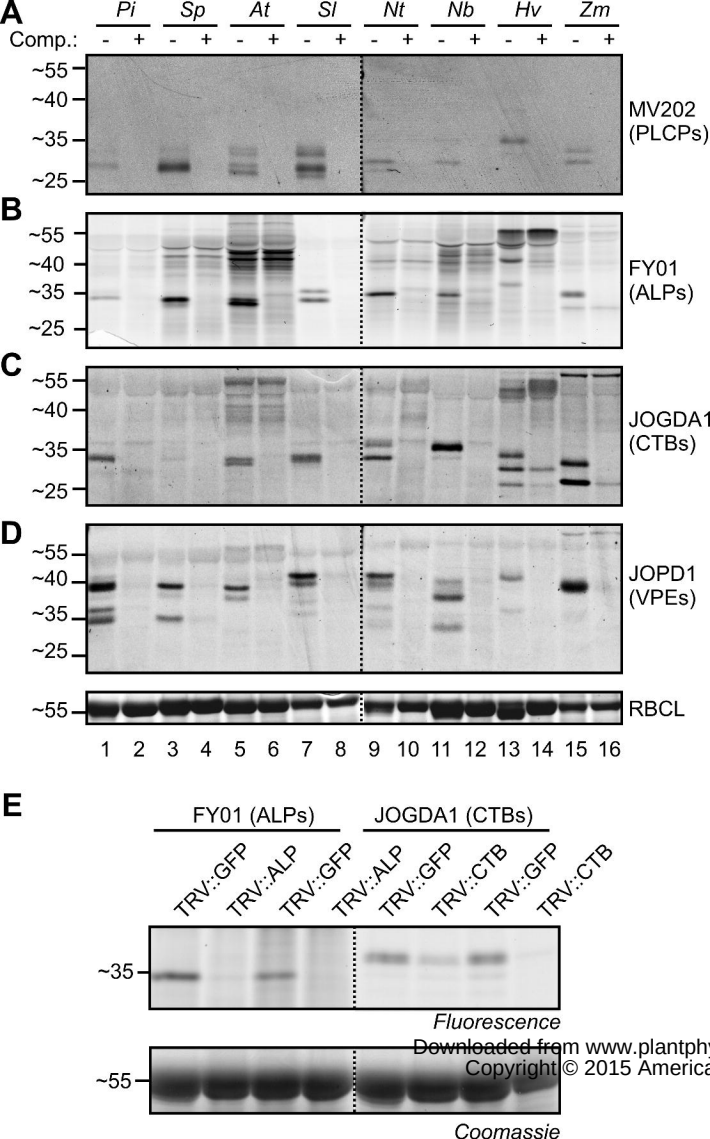

Downloaded from www.plantphy
Copyright © 2015 America

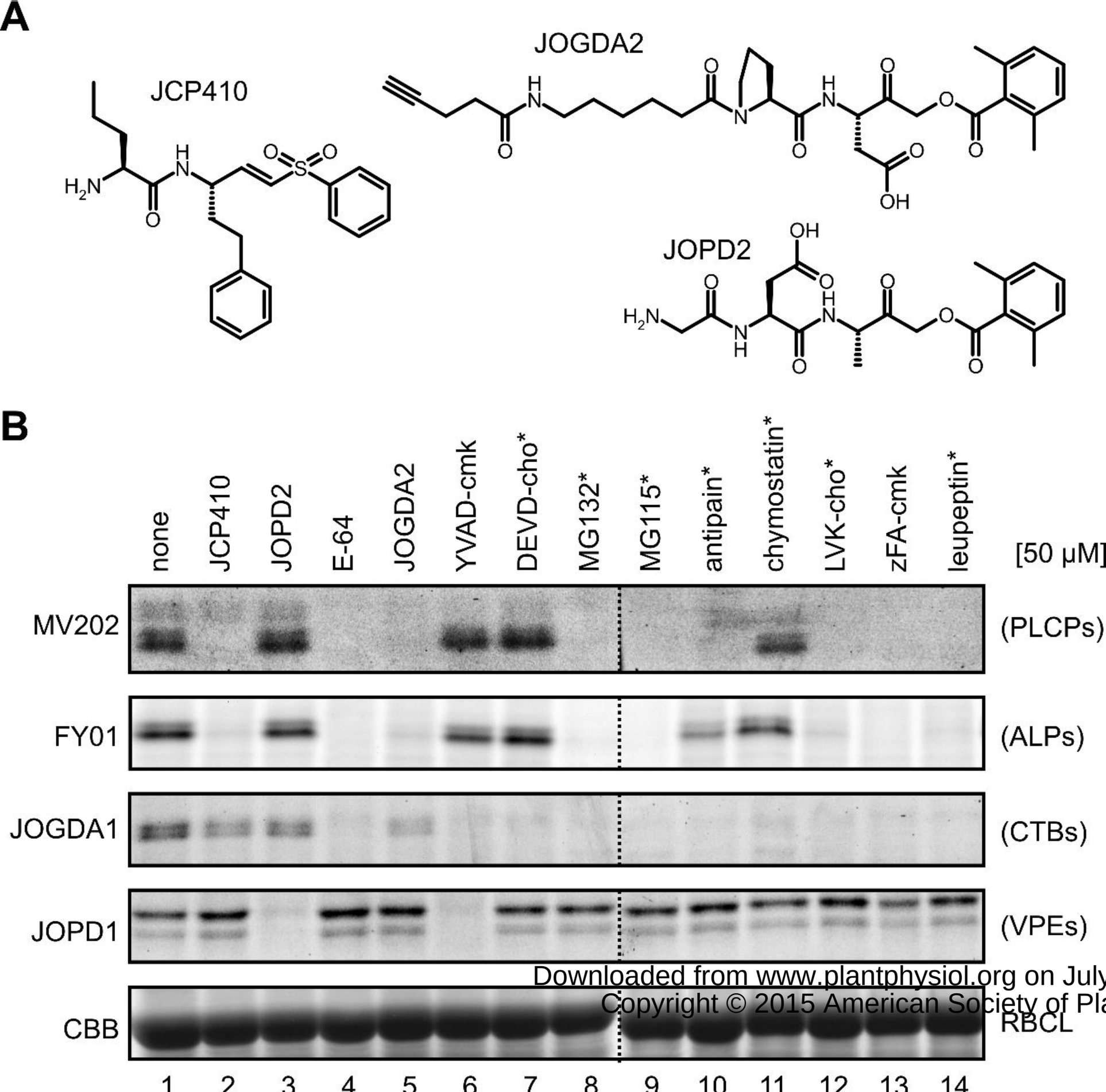

Downloaded from www.plantphysiol.org on July
Copyright © 2015 American Society of Pla

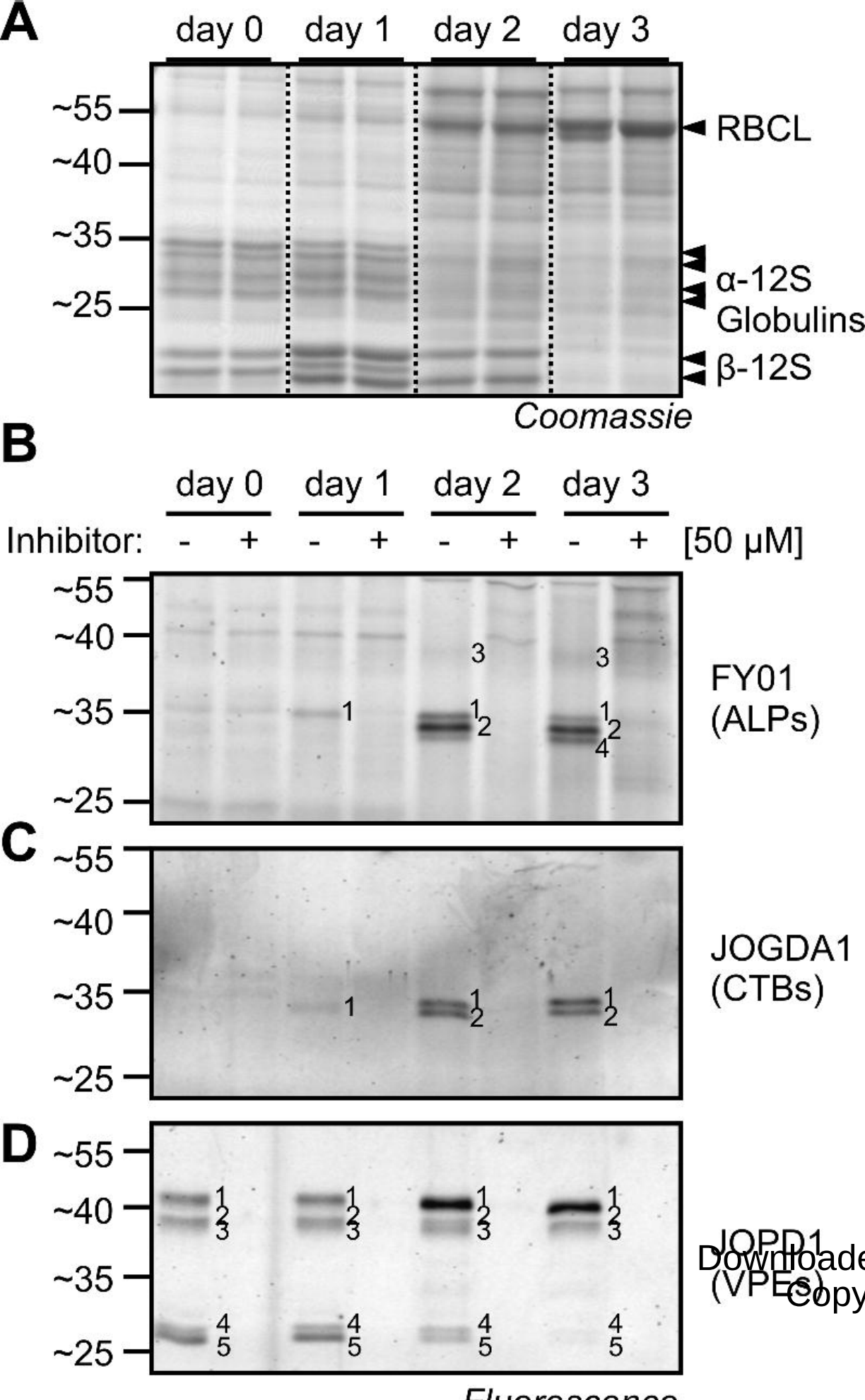

Downloade
Copy

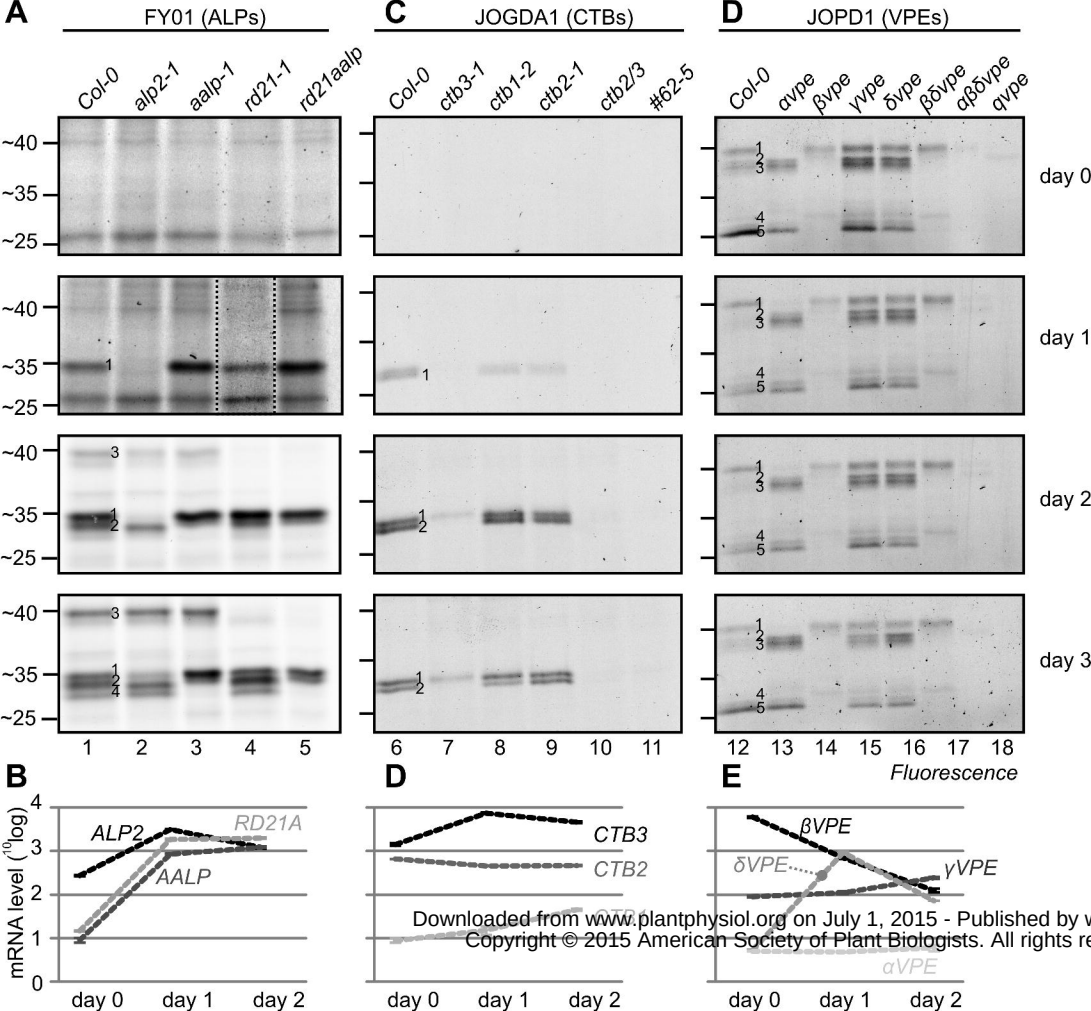

Downloaded from www.plantphysiol.org on July 1, 2015 - Published by w
Copyright © 2015 American Society of Plant Biologists. All rights re

Supplemental File S1: Chemical synthesis of AOMK probes

For synthesis of the AOMK probes, a solid phase-based approach was used following essentially protocols by Kato *et al*. (*Nat. Chem. Biol.* **2005**, *1*, 33-38).

Synthesis of GDA-AOMK probes

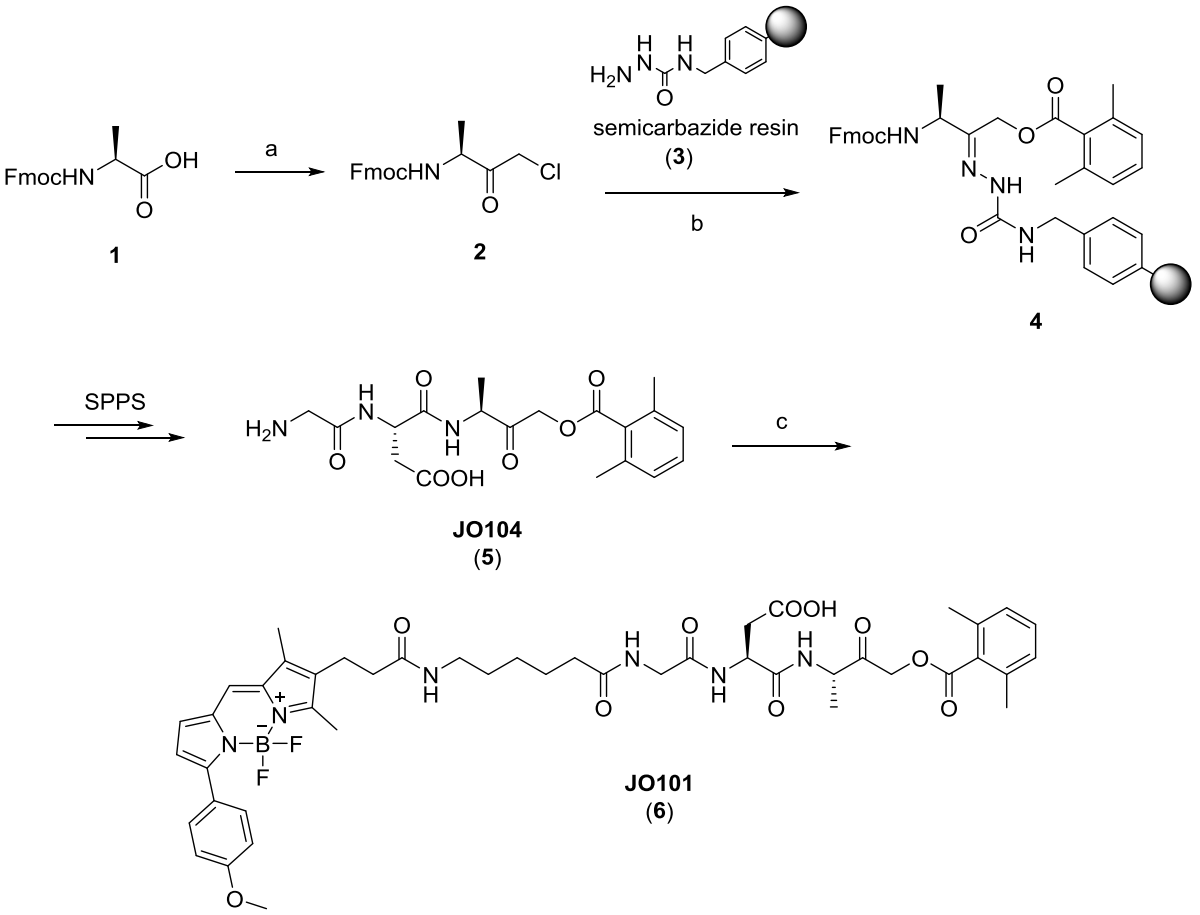

Scheme 1. Chemical synthesis of the GDA-AOMK probes **JOGDA1** (**6**) and **JOGDA2** (**5**). a) i) *iso*-butyl chloroformate (1.15 eq.), NMM (1.25 eq.), THF, -10 °C, 25 min, ii) diazomethane (4 eq.), 0 °C to rt, 3 h, iii) aq. conc. HCl/AcOH (1:1), 0 °C, 1 h; b) semicarbazide resin **3**, 2,6-dimethyl benzoic acid (3.75 eq.), KF (7.5 eq.), DMF; c) Bodipy-Ahx-NHS (0.33 eq.), DIEA (17.5 eq.), DMF, rt, 16 h.

Synthesis of Fmoc-Ala-CMK (2)

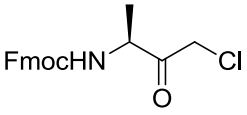

A 0.2 M solution of Fmoc-Ala-OH (1.65 g, 5 mmol) in anhydrous THF was stirred in an ice/acetone bath at -10 °C. To this solution, *N*-methylmorpholine (686 µL, 6.25 mmol, 1.15 eq.) and *iso*-butyl chloroformate (752 µL, 5.75 mmol, 1.25 eq.) were sequentially added, resulting in the formation of a white precipitate. The reaction mixture was stirred for additional 25 min at -10 °C. The required diazomethane was generated *in situ* using the procedure described in the Aldrich Technical Bulletin (AL-180). This ethereal diazomethane solution (20 mmol, 4 eq.) was transferred to the stirred solution of the mixed anhydride at 0 °C and the resulting reaction mixture was allowed to warmed to room temperature over 3 h. To obtain the desired chloromethyl ketone, a solution of concentrated hydrochloric acid and acetic acid (1:1, 15 mL) was then added dropwise to the reaction mixture at 0 °C and stirred for 1 h. Ethyl acetate was added, the organic layer was separated, washed with water, brine, sat. aq. $NaHCO_3$ solution, dried over Na_2SO_4 and evaporated to dryness, yielding 1.82 g (>98%) of **2** in sufficient purity for the next synthetic manipulations.

^{1}H NMR ($CDCl_3$) δ 7.77 (d, *J* = 7.5 Hz, 2H), 7.57 (dd, *J* = 18.6, 14.1 Hz, 2H), 7.41 (t, *J* = 7.5 Hz, 2H), 7.32 (td, *J* = 7.4, 1.0 Hz, 2H), 5.38 (d, *J* = 6.5 Hz, 1H), 4.67 – 4.54 (m, 1H), 4.45 (ddd, *J* = 29.4, 10.6, 7.0 Hz, 2H), 4.22 – 4.17 (m, 2H), 1.45 – 1.27 (m, 3H); **^{13}C NMR** ($CDCl_3$) δ 201.70, 155.83, 143.78, 141.47, 127.92, 127.22, 125.15, 125.06, 120.15, 67.06, 53.61, 47.32, 46.10, 27.73, 18.84, 17.63; **LC-MS** (ESI): t_R = 9.29 min, 344.10 calcd. for $C_{19}H_{19}ClNO_3^+$ $[M+H]^+$, found 344.61.

Synthesis of semicarbazide resin 3

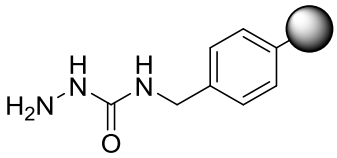

Aminomethylpolystyrene resin (0.5 g, 0.45 mmol/g) was dried under vacuum overnight in a 10 mL-polypropylene cartridge. The resin was presolvated with DMF for 30 min, the solvent was removed by filtration and a presolvation step with DCM for additional 30 min was performed. A 1 M solution of *N*, *N*'-carbonyldiimidazole (0.8 g, 4.95 mmol, 11 eq.) in DCM was added to the resin and the resin was shaken at room temperature for 3 h. The reagent was drained and the resin was washed with DCM followed by DMF. A 10 M solution of hydrazine (1.55 mL, 49.5 mmol, 110 eq.) in DMF was added to the resin, and the resin was shaken at room temperature for 1 h. The resin was washed with DMF followed by DCM, dried in vacuo, and stored until further use at 4 °C.

Synthesis of resin bound Fmoc-Ala-AOMK (4)

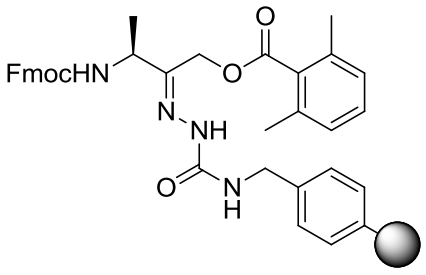

A 0.5 M solution of Fmoc-Ala-CMK (**2**, 0.2 g, 0.585 mmol) in DMF was added to the resin. The cartridge was tightly sealed and shaken at 50 °C for 3 h. The resin was washed with DMF. A 0.5 M solution of 2,6-dimethylbenzoic acid (170 mg, 2.2 mmol, 3.75 eq.) and potassium fluoride (128 mg, 4.4 mmol, 7.5 eq.) in DMF was added to the resin. The resulting suspension was shaken at room temperature overnight. After the solution was removed from the resin, the resin was washed with DMF followed by DCM, and dried in vacuo. The loading of the resin was determined as 0.3 mmol/g *via* the Fmoc loading assay.

Synthesis of H-GDA-AOMK (JO104, 5)

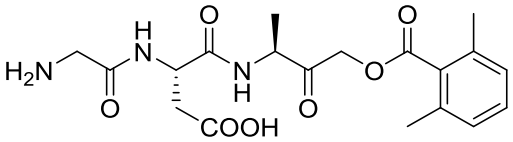

This AOMK probe was obtained from resin **4**, using standard solid phase peptide synthesis. To this end, the following general coupling conditions were used: All amino acid couplings were performed in a syringe reactor, using commercially available Fmoc-amino acids (4 eq.), HOBt (4 eq.), HBTU (4 eq.) and DIEA (4 eq.) in DMF at room temperature with a coupling time of 2 h. High coupling rates of the different coupling steps was verified by Kaiser tests. Fmoc cleavages were performed with 20% piperidine in DMF for 15 min. After each coupling or Fmoc cleavage step, the resin was washed six times with DMF. Cleavage from the resin and simultaneous deprotection of amino acid side-chains was achieved by agitation of the resin for 2 h in a cleavage solution containing 95% TFA, 2.5% TIS and 2.5% H_2O. The cleavage-solution, containing the desired product, was collected and the resin was rinsed twice more with the cleavage solution. The combined solutions were evaporated to dryness and the crude product was purified by RP-HPLC.

LC-MS (ESI): t_R = 5.07 min, 408.17 calcd. for $C_{19}H_{26}N_3O_7^+$ $[M+H]^+$, found 408.37.

Synthesis of Bodipy-GDA-AOMK (JOGDA1, 6)

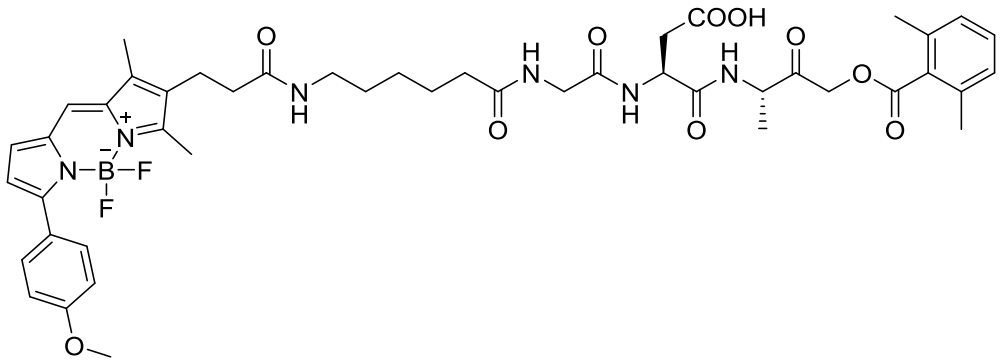

Due to the high price of commercial Bodipy-Ahx-NHS, we used this component as the limiting factor in this step. H-GDA-AOMK (**JOGDA2**, 2 mg, 4.9 µmol) was dissolved in DMF (0.5 mL) and DIEA (5 µL, 3.7 mg, 17.5 eq.) and a solution of Bodipy-Ahx-NHS (1 mg, 1.64 µmol) in DMF (0.5 mL) was added. The resulting reaction mixture was stirred for 16 h at rt. Afterwards, all volatiles were removed *via* reduced pressure and the crude product was purified by RP-HPLC, yielding 1.46 mg (1.62 µmol, 99%) of the desired product **JOGDA1** (**6**).

LC-MS (ESI): t_R = 8.64 min, 923.39 calcd. for $C_{46}H_{55}BF_2N_6NaO_{10}^+$ $[M+Na]^+$, found 923.45.

Synthesis of PD-AOMK probes

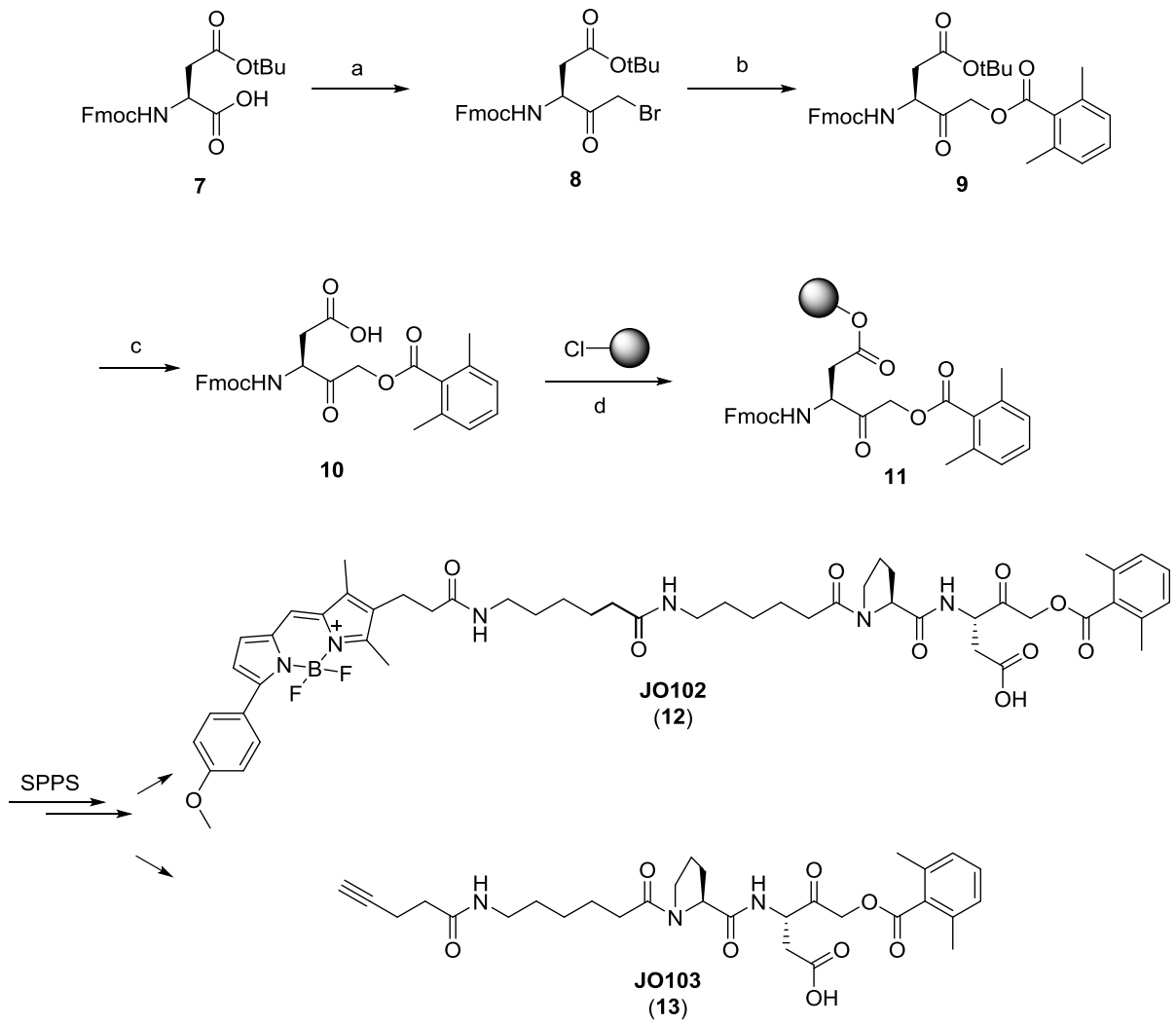

Scheme 2. Chemical synthesis of PD-AOMK probes **JOPD2** (**12**) and **JOPD2** (**13**). a) i) *iso*-butyl chloroformate (1.15 eq.), NMM (1.25 eq.), THF, -10 °C, 25 min, ii) diazomethane (4 eq.), 0 °C to rt, 3 h, iii) 30% HBr in AcOH, 0 °C, 1 h; b) 2,6-dimethyl benzoic acid (1.2 eq.), KF (3 eq.), DMF, 0 °C, overnight; c) TFA/DCM (1:4), rt, 1 h; d) 2-chloro trityl resin (0.83 eq.), DIEA (5 eq.), DCM, rt, 12 h.

Synthesis of Fmoc-Asp(O*t*Bu)-BMK (8)

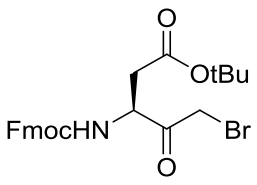

A 0.2 M solution of Fmoc-Asp(*t*Bu)-OH (2 g, 5 mmol) in anhydrous THF was stirred in an ice/acetone bath at -10 °C. To this solution, *N*-methylmorpholine (686 µL, 6.25 mmol, 1.15 eq.) and *iso*-butyl chloroformate (752 µL, 5.75 mmol, 1.25 eq.) were sequentially added, resulting in the formation of a white precipitate. The reaction mixture was stirred for additional 25 min at -10 °C. The required diazomethane was generated *in situ* using the procedure described in the Aldrich Technical Bulletin (AL-180). This ethereal diazomethane solution (20 mmol, 4 eq.) was transferred to the stirred solution of the mixed anhydride at 0 °C and the resulting reaction mixture was allowed to warmed to room temperature over 3 h. To obtain the desired bromomethyl ketone, a solution of 30% HBr in acetic acid (10 mL) was then added dropwise to the reaction mixture at 0 °C and stirred for 1 h. Ethyl acetate was added, the organic layer was separated, washed with water, brine, sat. aq. $NaHCO_3$ solution, dried over Na_2SO_4 and evaporated to dryness, yielding 2.4 g (>98%) of **8** in sufficient purity for the next synthetic manipulations.

Synthesis of Fmoc-Asp(O*t*Bu)-AOMK (9)

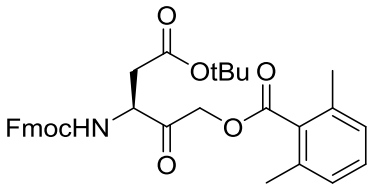

A 0.2 M solution of **8** (2.4 g, 5 mmol) in DMF was stirred at 0 °C. To this solution, potassium fluoride (870 mg, 15 mmol, 3 eq.) and 2,6-dimethylbenzoic acid (900 mg, 6 mmol, 1.2 eq.) were added. The reaction mixture was allowed to warm to room temperature and stirred overnight. It was diluted by addition of ethyl acetate, the organic layer was separated and washed with water, brine, sat. aq. $NaHCO_3$ solution and dried over $MgSO_4$. The solvent was removed under reduced pressure and the residue was purified by silica gel chromatography (ethyl acetate/cyclohexane = 1:5) to obtain 1.65 g (60%) of pure product **9** as a white solid.

TLC (ethyl acetate/cyclohexane = 1:5): R_f = 0.2; **^{1}H NMR** ($CDCl_3$) δ = 7.82 (d, *J* = 8.2 Hz, 2H), 7.63 (m, 2H), 7.41 (m, 2H), 7.33 (m, 2H), 7.20 (t, *J* = 7.6 Hz, 1H), 7.04 (d, *J* = 7.64 Hz, 2H), 5.89 (d, *J* = 8.8 Hz, 1H), 5.07 (q, *J* = 16.8 Hz, 3H), 4.65 (m, 2H), 4.24 (t, *J* = 6.44 Hz, 1H), 2.97 (dd, *J* = 17.1, 4.88 Hz, 1H), 2.91 (dd, J = 17.1, 4.88 Hz, 1H), 2.40 (s, 6H), 1.45 (s, 9H); **^{13}C NMR** ($CDCl_3$) δ = 201.1, 169.0, 156.2, 143.7, 141.5, 141.5, 135.8, 132.7, 129.8, 127.9, 127.8, 125.2, 120.2, 120.2, 82.4, 67.3, 66.8, 54.9, 47.4, 36.7, 28.1, 27.1, 20.0; **LC-MS** (ESI): t_R = 11.44 min, 580.23 calcd. for $C_{33}H_{35}NNaO_7^+$ $[M+Na]^+$, found 580.11.

Synthesis of Fmoc-Asp-AOMK (10)

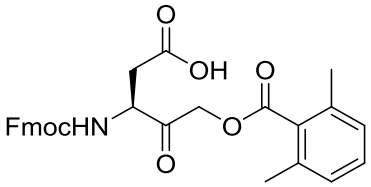

Fmoc-Asp(O*t*Bu)-AOMK (**9**, 1.65 g, 2.96 mmol) was dissolved in TFA/DCM (1:4, 15 mL) and stirred for 1 h at room temperature. The reaction mixture was diluted by addition of DCM, sufficient amounts of toluene were added and the cleavage solution was removed by co-evaporation. The product was dried *in vacuo*. The crude product **10** was used without further purification.

LC-MS (ESI): t_R = 9.70 min, 524.16 calcd. for $C_{29}H_{27}NNaO_7^+$ $[M+Na]^+$, found 524.37.

Synthesis of resin-bound Fmoc-Asp-AOMK (11)

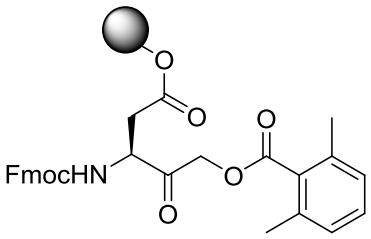

2-Chlorotrityl resin (500 mg, 0,685 mmol, maximal loading of 1.37 mmol/g) was loaded with Fmoc-Asp-AOMK (**10**, 420.8 mg, 0.84 mmol, 1.2 eq.) in the presence of DIEA (731 µL, 4.1 mmol, 6 eq.) in dry DCM (8 mL) under an argon atmosphere for 12 h at room temperature. It was washed 3x with DCM and 3x with DMF, capped for 30 min by addition of DCM/MeOH/DIEA (17 : 1 : 2 ,15 mL). The resin was washed again 5x with DMF and 5x with DCM and was subsequently dried under high vacuum. The resulting loading of the resin was determined as 0.49 mmol/g *via* the Fmoc loading assay.

General procedure for the SPPS to JOPD2 (12) and JOPD2 (13)

The AOMK probes were assembled by solid phase synthesis. To this end, the following general conditions were used: All amino acid couplings were performed in a syringe reactor, using commercially available Fmoc-amino acids (4 eq.) or 4-pentynoic acid (4 eq.), HOBt (4 eq.), HBTU (4 eq.) and DIEA (4 eq.) in DMF at room temperature with a coupling time of 2 h. For coupling of the Bodipy-Ahx moiety, commercially available Bodipy-Ahx-OSu reagent (1 eq.) was however used. High coupling rates of the different coupling steps was verified by Kaiser tests. Fmoc cleavages were performed with 20% piperidine in DMF for 15 min. After each coupling or Fmoc cleavage step, the resin was washed six times with DMF. Cleavage from the resin and simultaneous deprotection of amino acid side-chains was achieved by agitation of the resin for 2 h in a cleavage solution containing 95% TFA, 2.5% TIS and 2.5% H_2O. The cleavage-solution, containing the desired product, was

collected and the resin was rinsed twice more with the cleavage solution. The combined solutions were evaporated to dryness and the crude product was purified by RP-HPLC.

Synthesis of Bodipy-PD-AOMK (JOPD1, 12)

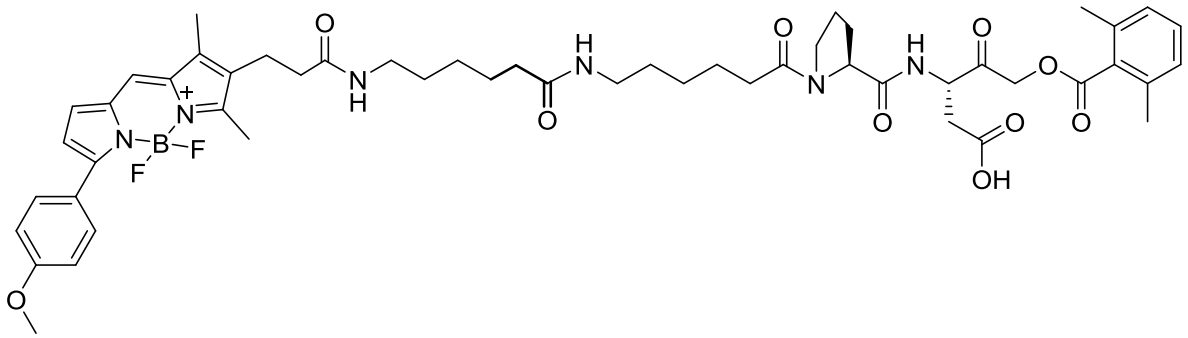

Following the above protocol for SPPS led to 0.82 mg of the product **JOPD1** as a yellowish solid.

LC-MS (ESI): t_R = 8.71 min, 963.48 calcd. for $C_{52}H_{65}BFN_6O_{10}^+$ $[M+H]^+$, found 963.52.

Synthesis of pent-4-ynoic-PD-AOMK (JOPD2, 13)

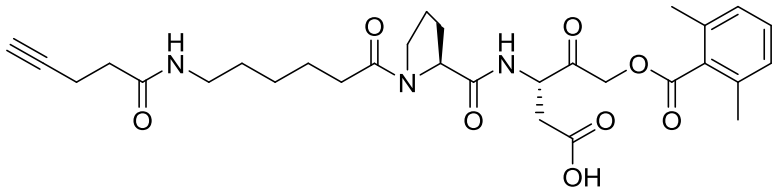

Following the above protocol for SPPS led 4.4 mg of the product **JOPD2** as a colorless solid.

LC-MS (ESI): t_R = 6.93 min, 570.28 calcd. for $C_{30}H_{40}N_3O_8^+$ $[M+H]^+$, found 570.24.

Supplemental Figures Lu et al., '*Subfamily-specific Fluorescent Probes for Cys proteases Display Dynamic Protease Activities During Seed Germination'*

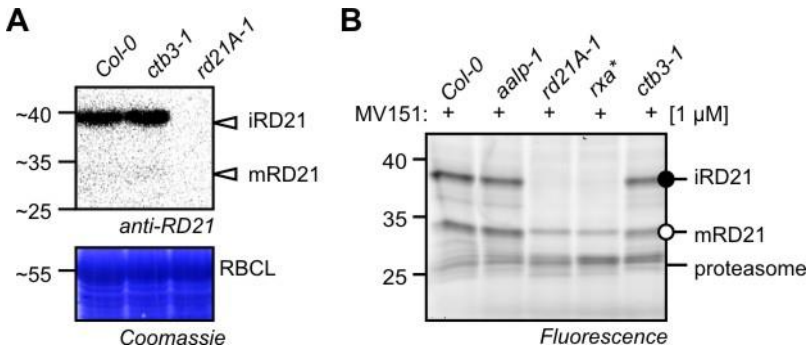

Supplemental Figure S1 Accumulation and labeling of RD21 in *ctb3-1* mutant plants.

(A) RD21 processing and accumulation is unaltered in *ctb3-1* mutant. Leaf extracts of WT plants, *rd21A-1* and *ctb3-1* were separated on protein gels, transferred to PVDF and probed with the primary anti-RD21 antibody and secondary anti-rabbit antibody.

(B) RD21 activity is unaltered in the *ctb3-1* mutant. Labeling profile of MV151 on leaf extracts of various protease mutants. MV151 labels both RD21 and the proteasome (Gu et al., (2010) Plant J. 62, 160-170). Leaf extracts of Col-0, *aalp-1, rd21A-1, rxa** (*, double mutant *rd21A-1 x aalp-1*) and *ctb3-1* were labeled with 1 µM MV151 at pH 6 and labeled proteins were detected by in-gel fluorescence. MV151 labels mature RD21 (mRD21) at 34 kDa and this signal is unaffected in the *ctb3-1* mutant.

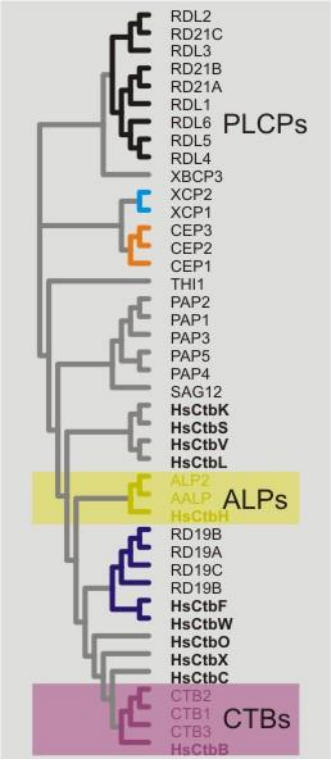

Figure S2. Phylogenetic tree of human and Arabidopsis PLCPs

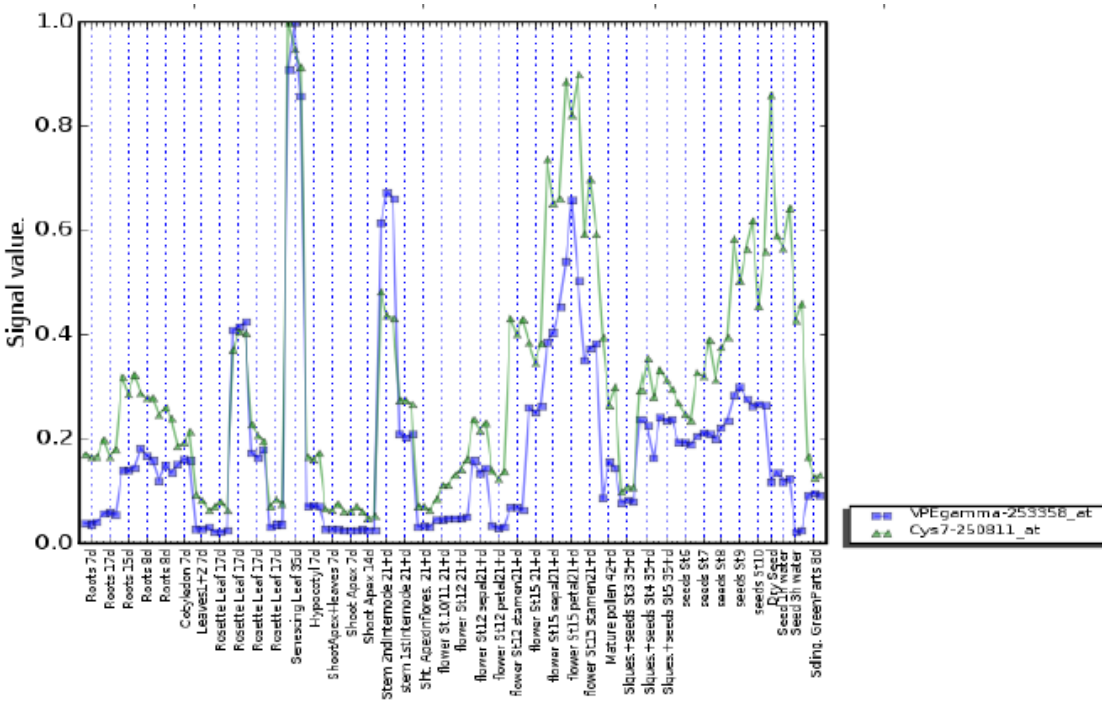

Figure S3. Co-expression of *AtCYS6* with *γVPE* during development.

Data were extracted from *Arabidopsis thaliana* microarrays using Genevestigator.